SYNTHESIS OF WATER SOLUBLE TERPYRIDINE-LIGANDS TO STUDY AND OPTIMIZE ITS USE IN BIOIMAGING

By
Kiante Raqui Graham

A Thesis

Submitted to the
Faculty of the Graduate School
of
Western Carolina University
in Partial Fulfillment of
the Requirements for the Degree
of
Master of Science

Director: Dr. Brian Dinkelmeyer, Organic Chemistry, Department of Chemistry & Physics

November 2024

Acknowledgements

I would like to acknowledge my advisor Dr. Brian Dinkelmeyer and my committee members Dr. Al Fischer and Dr. Jamie Wallen for helping me in completion of my thesis. I want to like to also thank the Chemistry and Physics department. I want to also acknowledge Matt Burleson for training me on multiple instruments and answering my questions. Thank you to Dr. Robert Youker for helping me with the confocal microscope images. Also thank you to the Graduate School for funding my research during the summer with the Summer Research Assistantship. Also, I want to say thank you to my peers and grad school mates for their friendship. I especially give thanks to my family for believing in me. I want to thank Dr. Dinkelmeyer for helping me every step of the way, without you I don't know what I would have done.

TABLE OF CONTENTS

Pages

LIST OF FIGURES

Pages

LIST OF GRAPHS

Pages

v

LIST OF SCHEMES

Pages

ABSTRACT

Synthesis of Water Soluble Terpyridines-Ligands to Study and Optimize its use in Bioimaging.
Kiante Raqui Graham, M.S.
Western Carolina University (November 2024)
Director: Dr. Dinkelmeyer

Pyrophosphate (**PPi**) anions play an important role in many biological and cellular metabolic processes. **PPi** anion is a potentially useful indicator of metabolic function, ATP hydrolysis, and diseases such as calcium pyrophosphate dihydrate crystal deposition disease. This research develops a highly selective probe for detecting **PPi** in water at the nanomolar level using simple zinc dichloride terpyridine complexes, applicable in diagnostics and medicine. Terpyridines (**L**) and their **$ZnCl_2L$** complexes were synthesized. The **L** synthesizes compounds in the presence of an R-group, which enhances water solubility or fluorescence for **PPi** detection. The **L** and **$ZnCl_2L$** complexes were characterized by ^{1}H and ^{13}C NMR, FTIR, confocal microscopy, and fluorescence spectroscopy. Fluorescence titrations of **$ZnCl_2L$** complexes were performed with varying **PPi** concentrations. The maximum fluorescence intensity occurred at a 3:1 mole ratio of **$ZnCl_2L$** to **PPi.** . It was found that terpyridine- **$ZnCl_2L$** complexes bind specifically with **PPi** and form fluorescent nanoaggregates. The structure of the **L** significantly affected their luminescence properties. Para-substituent that were with either electron donating or withdrawing significantly changed the fluorescent intensity of the terpyridine complexes. The ligands (**L_1, L_2, L_4**) contain sp^3 nitrogen at the para position, which acts as a strong electron-donating group, fluoresce intensely. The **$ZnCl_2L_2$** shows a higher intensity compared to **$ZnCl_2L_1$** and **$ZnCl_2L_4$**. The **$ZnCl_2L_4$**, was not used in the confocal microscope imaging due to its low fluorescence intensity compared to the other complexes. We sought to assess the effectiveness of **$ZnCl_2L_{1-2}$** complexes in confocal microscope imaging and compare their ability to successfully stain HEK293 cells for fluorescence imaging by binding to the **PPi** anion within the nucleus.

CHAPTER 1: INTRODUCTION

1.1 BACKGROUND

PPi anions have been studied intensely since the 1960s due to their considerable role in cellular metabolic processes and several diseases**Error! Bookmark not defined.**. These **PPi** anions are typically found in ATP and other nucleotide triphosphates, which can be found in DNA or RNA. They are typically formed by hydrolysis of ATP into AMP in cells during DNA replication. A phosphodiester bond forms between the incoming deoxynucleotide triphosphate (dNTP) and the terminal primer nucleotide, releasing a **PPi** anion group[1]. The formation of a phosphodiester bond between the incoming deoxynucleotide triphosphate(dNTP) and the terminal primer nucleotide results in the release of a **PPi** anion.[1] The released **PPi** has been considered important analyte to detect in recent cancer research as well as real-time sequencing of DNA**Error! Bookmark not defined.** (**Figure 1**). The **PPi** anion has the potential to be a useful indicator of metabolic function and diseases.

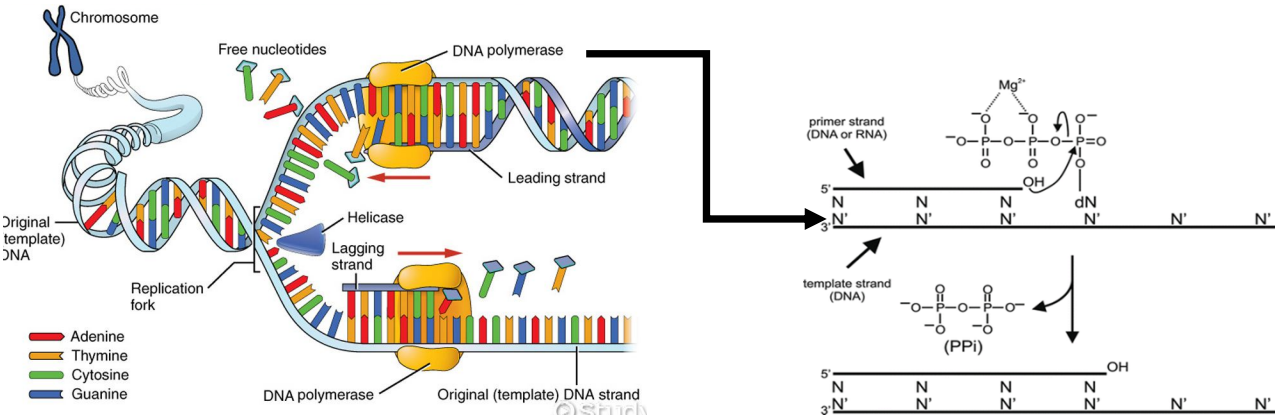

Figure 1. DNA polymerase catalyze the formation of a phosphodiester bond (**PPi-PPi**) between the incoming deoxynucleotide triphosphate(dNTP) and the terminal primer nucleotide with the release of a **PPi** group.

Up to now, methods for detection of **PPi** anions are mainly chemiluminescence, enzymatic techniques, capillary electrophoresis, electrochemical sensing, as well as spectrofluorometry[2]. Since **PPi** anions have an extremely low detection limit under physiological environments, detecting them using fluorescence-based methods proves to be a very challenging task. Their low detection limit has necessitated the use of fluorescent molecules to detect **PPi** anions. Fluorescent molecules require two necessary parts: a receptor that binds specifically the **PPi** anion[2] and a fluorophore that emits upon binding. Terpyridine(**L**) are promising candidates that have been extensively studied due to their luminescent properties, which are used for the fluorescence recognition of targets, and their versatility in supramolecular assemblies and polymers[2]. Terpyridine **L** coordinates easily with transition metals and form a particularly bright fluorescent complex with zinc in comparison to other transition metals. (**Figure 2.).**

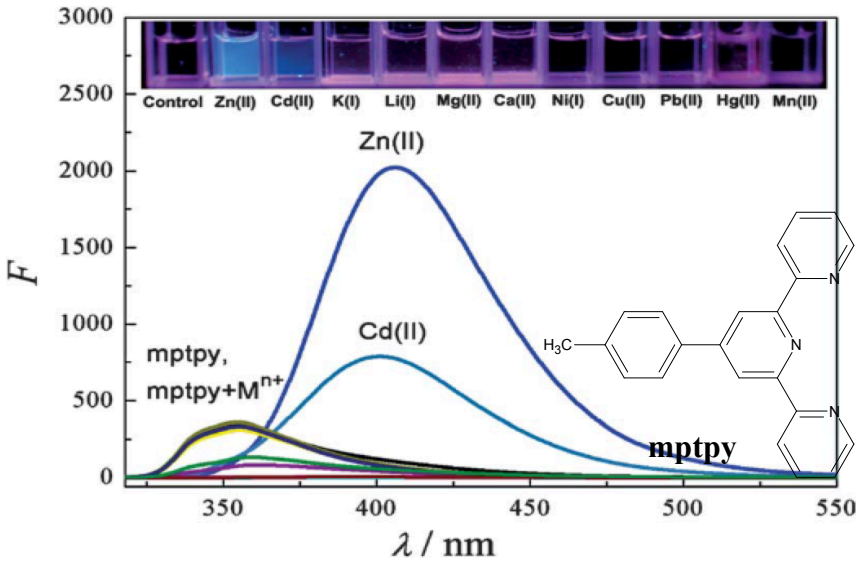

Figure 2. Fluorescence spectra of in the absence and presence of various metal cations in an ethanol/water (1:3, v/v) solution. Inset is the photograph taken under UV irradiation (256nm). Concentration 4-(Methylphenyl)-2,2';6',2"-terpyridine 75mM; metal ions, 75mM; excitation 280nm**Error! Bookmark not defined.**.

Another benefit of using zinc is that it is benign to living cells at low concentrations. Zinc is an important trace metals for human beings and plays an important role in the regulation of the cellular metabolism, its cytoprotective effect, and its ability to suppress the apoptotic pathways[1]. Additionally, zinc has a high affinity and specificity for **PPi** anions, which is shown in **Figure 3** and **Figure 4**.

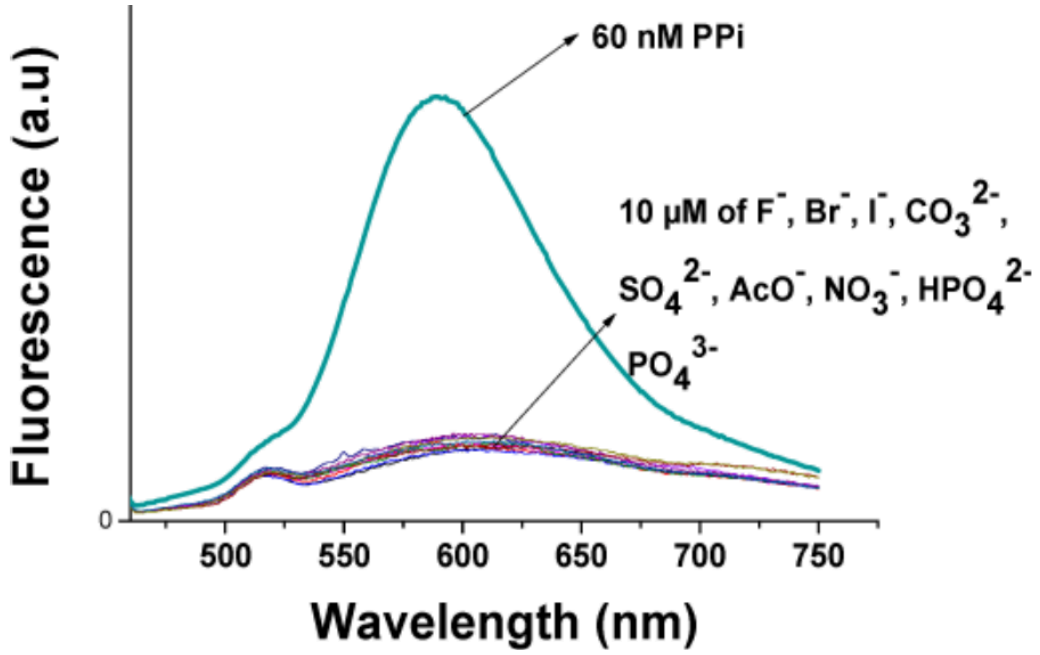

Figure 3. Emission of zinc dichloride 4-(dimethyaminolphenyl)-2,2';6',2"-terpyridine (**$ZnCl_2L_1$**) (50μM) in 10 mM HEPES buffer (pH 7.4) in presence of different anions**Error! Bookmark not defined.**.

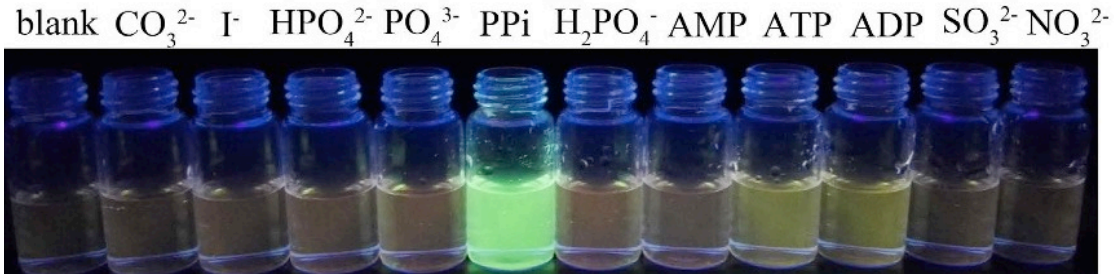

Figure 4. Diagram of **$ZnCl_2L$** complexes underneath a 365nm UV lamp showing the selectivity for **PPi** anion over different biological anions [2].

Zinc dichloride terpyridine (**$ZnCl_2L$**) complexes bind **PPi** to form fluorescent nanoaggregates. Aggregation-induced emission (AIE) creates an intense turn-on fluorescence response. The **$ZnCl_2L$** complexes' high kinetic and thermodynamic stability confer unique properties, but the main reason they are commonly observed is the ease of synthesizing derivatives with various substituents, particularly at the 4′-position of the central ring**Error! Bookmark not defined.**. The most common synthesis of these complexes is based on the Knöhnke synthesis (**Scheme 1**).

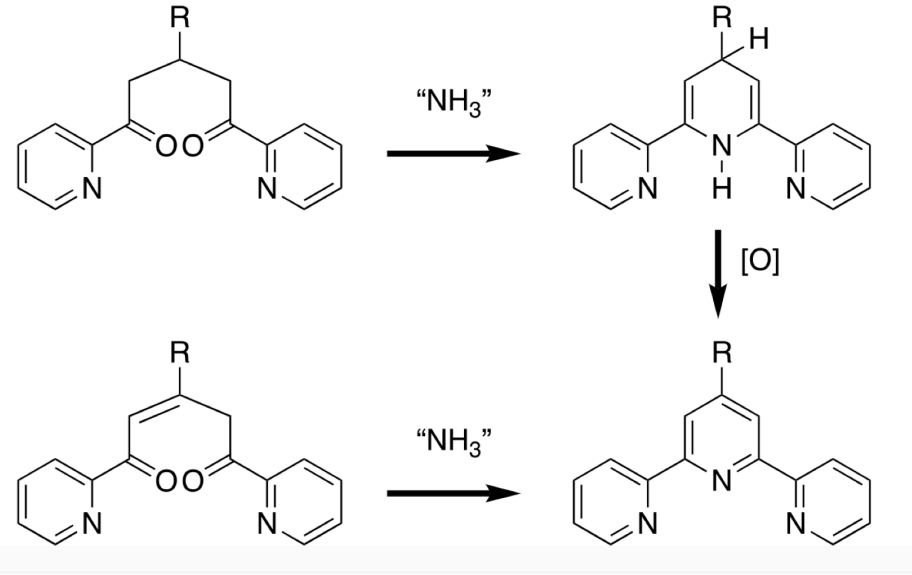

Scheme 1. The typical synthetic strategy for a 2,2′:6′,2″-tpy involves the cyclization of 1,5-bis(pyridin-2-yl)pentane-1,5-dione or 1,5-bis(pyridin-2-yl)pent-2-ene-1,5-dione or equivalent with ammonia[3].

Zinc dichloride terpyridine (**$ZnCl_2L$**) complexes meet the two requirements needed for fluorescent molecules. The **$ZnCl_2L$** complexes have the ability to emit a fluorescence signal and can bind to the **PPi** anion. The aromatic rings in **$ZnCl_2L$** are capable of intermolecular π-π stacking interactions**Error! Bookmark not defined.**. Solid samples of **$ZnCl_2L$** complexes can

fluoresce on their own, but their fluorescence emission is quenched once they are dissolved in water.

By combining **$ZnCl_2L$** complexes and **PPi** under appropriate conditions, they can form aggregates. In this AIE system, the aggregates can produce more intense fluorescence response than their individual parts. Aggregates are formed whenever single nanoparticles cluster together to form a larger object. There are many mechanisms that cause AIE, which involve the elimination of non-radiative processes. Some examples of non-radiative process include bond vibrations, molecular rotation, bond rotation and molecular collisions. One AIE mechanism involves the restriction of intramolecular rotation (RIR). The RIR mechanism describes how restriction of bond rotations can enhance fluorescence emission. The **$ZnCl_2L$** complexes can rotate at the position of the amine group, as well as the phenyl and pyridine (**Figure 5.**).

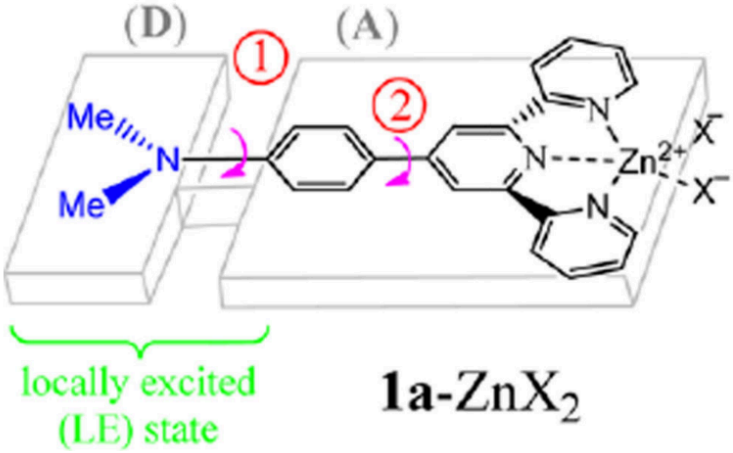

Figure 5. Illustrate LE and TICT state by (1)rotating of the amine group, and (2) phenyl and pyridine group[14].

The noncovalent intermolecular C-H π interactions help hold the aggregate-induced molecules together, stabilize the crystal packing, and restrict the rotational motions of the phenyl,

pyridine, and amine groups. The hindrance of the molecules' rotation can cause fluorescence "turn-on" systems. The intramolecular rotations of molecules can consume exciton energy, which is the energy needed for an electron or molecule to give off light, and the molecule can go through radiationless decay. Radiationless decay is a process where an atom or molecule transitions from an excited state to a lower energy state without emitting electromagnetic radiation (**Figure 6**). Once the molecules experience RIR in the places where the molecules rotate freely, it will trigger a light emission from the electrons of that molecule. This means that the exciton energy cannot be depleted by radiationless decay, making the electrons of that molecule more emissive.

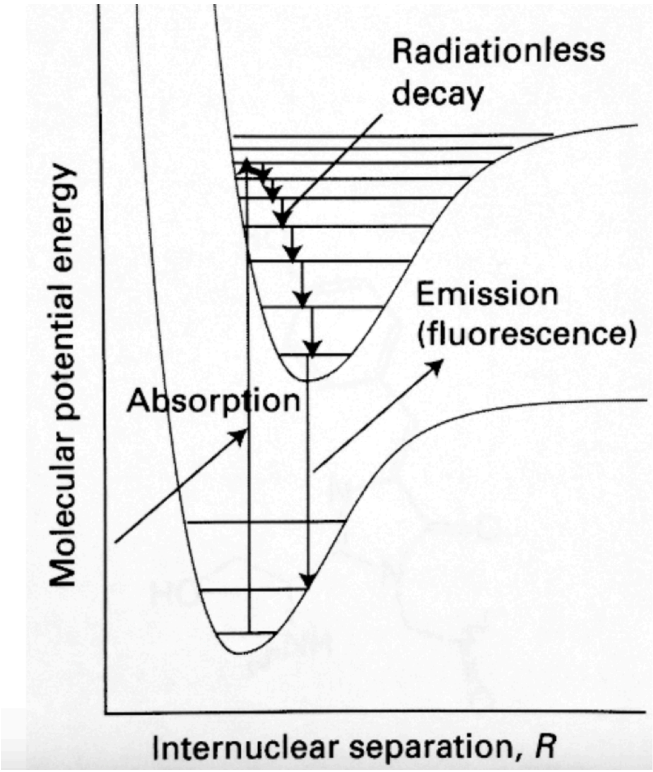

Figure 6. Morse potentials for two main quantum numbers. Source: Atkins' "Physical Chemistry", 9th ed, page 505.

A non-radiative process occurs when an electron reaches its lowest possible vibrational state before an electronic transition happens. The electron does not always relax directly to the lowest vibrational level. Upon absorption, the electron is often excited to a higher vibrational state rather than the lowest one. The energy lost during vibrational relaxation causes the emitted photon to have lower energy than the absorbed photon, which is shown in **Figure 6**. **$ZnCl_2L$** complexes bind well to **PPi** to produce an intense fluorescence response due to the electron donating/withdrawing nature of the R-group para-substituent on the **$ZnCl_2L$** complexes. This can have a large influence on their luminescent properties. The ligands on the **$ZnCl_2L$** complexes contained sp^3 nitrogen at the para position and act as strong electron donating groups (**Figure 7**). Conjugation of the nitrogen lone-pair electrons to the **L** pi-system is critical to the fluorescence behavior of the complexes. It is believed that the formation of the **PPi**-nanoaggregate enhances the fluorescence since the amine groups can no longer rotate freely and is locked into a conformation in which the lone-pairs are conjugated to the **L** π-system. The crystal structure of this complex, shown in **Figure 7**, reveals that the molecules have a conformation where the aromatic rings and nitrogen lone-pair are co-planar and aligned[5].

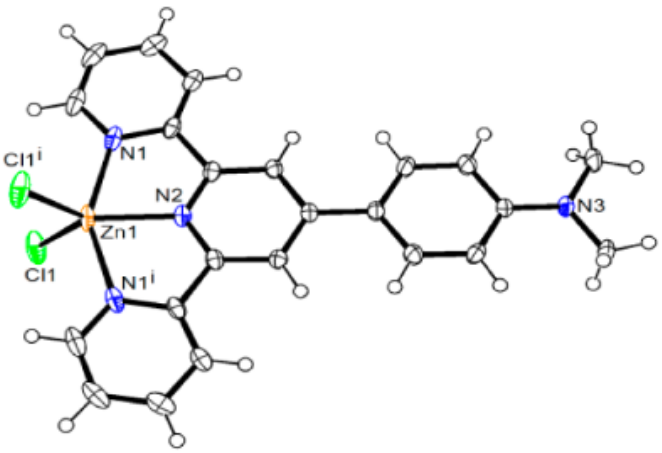

Figure 7. Crystal structure of a Zinc, dichloride (4-(4-N)-2,2′:6′,2″ terpyridine 3D structure.[4]

The **$ZnCl_2L$** complex, which contains empty coordination sites, has a greater tendency to bind with phosphates. This is especially evident with pyrophosphate (**PPi**) due to the stronger electrostatic interactions between the positively charged Zn(II) center and **PPi** compared to other phosphates. The strong affinity of **PPi** for the receptor **$ZnCl_2L$** explains this tendency. As a result, **$ZnCl_2L$** exhibited a specific response to **PPi**, enabling it to successfully differentiate **PPi** from other anions such as ATP and sodium phosphate (Pi) (Figure 8)**Error! Bookmark not defined.**.

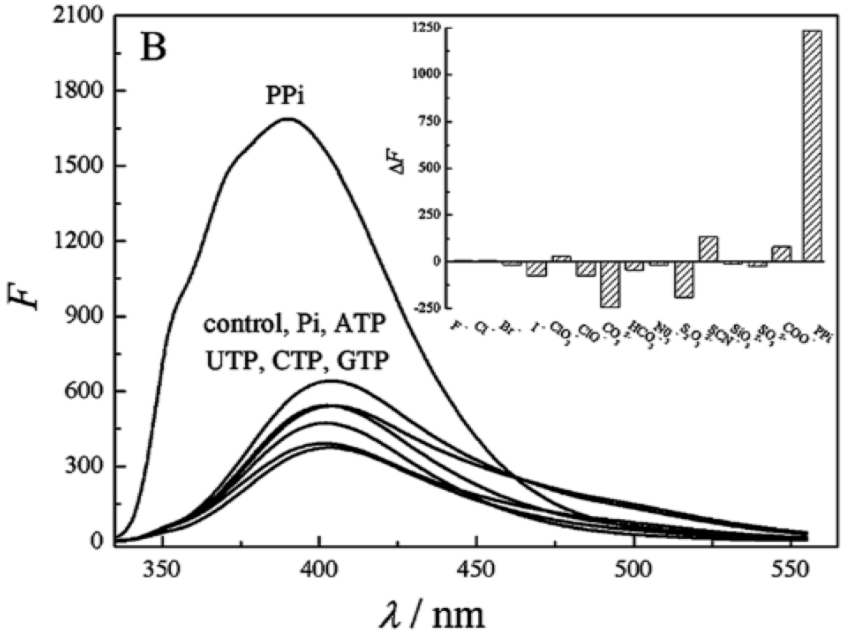

Figure 8. Emission at 388 nm shows the intensity changes of **$ZnCl_2L$** with various inorganic anions**Error! Bookmark not defined.**.

1.2 OBJECTIVES

In this research, we are focused on synthesizing simple **$ZnCl_2L$** with a variety of R-groups. Changing the R-group will affect the molecule's solubility, lipophilicity, and its binding

capabilities with **PPi**, as well as its fluorescence intensity. The objective of this project is to develop selective and sensitive probes for detecting **PPi** at the nanomolar level in water using **$ZnCl_2L$** complexes, and to investigate how **PPi** binding and fluorescence are affected.

CHAPTER 2: EXPERIMENTAL

General information and materials: All reagents and solvents were provided by WCU and purchase from commercial sources. ^{1}H and ^{13}C NMR spectra were obtain using Bruker Ascend 400 MHz. FTIR spectra were obtained using Perkin Elmer Spectrum One FTIR. Fluorescence spectra, excitation and emission were obtained using the SpectraMax iD5 multimode microplate reader.

Fluorescence titration Study: The receptor stock solution is prepared by adding 200µL of 25mM ZnCl2 in 100mL methanol to 2mL of 2.5mM L1-L4 in 25mL methanol in a 25mL volumetric flask and then diluting the resulting mixture with 50mL of 0.01M HEPES buffer at pH 7.4 in a 50mL volumetric flask. All solutions were sonicated for 5 minutes after mixing the receptor and the analyte.

Instrumentation for PPi Titration Studies: Fluorescence spectra and optimal wavelengths were obtained using the SpectraMax iD5 multimode microplate reader. It is capable of detecting and quantifying the light emitted from samples in the plate by exciting the molecule with light at a specific wavelength. The three settings on the instrument that are used to collect data are fluorescence spectrum, fluorescence endpoint, and spectral optimization wizard. The spectral optimization wizard is used to find optimal excitation and emission wavelengths for the ZnCl2L complexes. The excitation of the sample is important to achieve maximum fluorescence intensity. The fluorescence endpoint mode measures each well once at a single excitation and emission wavelength and gives an intensity value for each well. The fluorescence spectrum mode

measures the fluorescent spectrum for each well.

4-(4-dimethylyaminophenyl)-2,2':6',2"terpyrdine (L_1). 4-N,N-dimethylaminobenzaldehyde (0.7451g, 4.99mmol) was added to a solution of 2-acetylpyridine (1.21g, 1.08g/mL, 9.99mmol) in ethanol(20mL). Then NaOH pellets (0.569g, 1.42mmol) was added to the solution with vigorously stirring until the pellets dissolved completely. Concentrated NH_4OH (20mL, 28-30%) was added and the reaction was stirred at room temperature for 16 h. The precipitate was filtered and washed with ethanol. The crude product was recrystallized in methanol to produce a golden-yellow crystals. The low yield was due to loss of product during recrystallization processing. Yield: 0.1915g, 10.8% ^{1}H NMR (400MHz, $CDCl_3$) δ 3.04 (6H,s), δ 6.83 (2H,d, J=4.16Hz), δ 7.35 (2H,tt) δ 7.87 (4H,m). ^{13}C NMR (100MHz, DMSO) 40.36, 112.3, 117.5, 121.4, 123.6, 125.5, 128.1.

Zinc, dichloride (4-(4-dimethylyaminophenyl)-2,2':6',2"terpyrdine) ($ZnCl_2L_1$). 4-(4-dimethylyaminophenyl)-2,2':6',2" **L_1** (0.1987g, 0.5649mmol) was dissolved in dichloromethane (26.4mL) in an Erlenmeyer flask. A solution of $ZnCl_2$ (0.0894g, 0.656mmol) in methanol (25mL) was added to the flask and stir for 3h. The yellow precipitate was filter and washed with methanol. Yield: 0.1921g, 70% ^{1}H NMR (400MHz, $CDCl_3$) δ 3.05 (6H,s), δ 6.87-6.89 (2H,d, J=8.68Hz), δ 8.29 (2H,s), δ 8.20 (2H,d), δ 8.29 (2H,t), δ 8.79-8.93 (6H,m, J=10.92Hz, 37.6Jz, 4.04Hz). ^{13}C NMR (100MHz, DMSO) 40.36, 112.3, 117.5, 121.4, 123.6, 125.6, 128.1, 136.8, 149.1, 150.0, 151.1, 155.7, 156.7.

4-(4-morpholinephenyl)-2,2':6',2"terpyridine (L_2). 4-(4-Formylphenly)morpholine (1.9128g, 10mmol) and 2-acetylpyridine (2.4228g, 1.08g/mL, 20mmol) were combined in ethanol (75mL). KOH pellets (1.5491g) were added and the solution was stirred vigorously until pellets dissolved completely. NH_4OH (35mL, 28-30%) was added to the reaction mixture and stirred at room temperature for 24 h. The yellow precipitate was filter and wash with ethanol and water. The crude product was filtered from ethanol resulting in a bright yellow crystalline product. The low yield due is due to loss of product during recrystallization processing. The final product was a cotton textured bright yellow solid. Yield: 0.5027g, 12.7% ^{1}H NMR (400MHz, $CDCl_3$) δ 7.04-7.06 (2H,d, J=8.88Hz) δ 7.36-7.39 (2H,m) δ 3.91-3.94 (4H,t, J=4.76Jz) δ 8.68-8.70 (2H,d, J=7.96Hz) δ 7.87-7.92 (4H,m), δ 8.73-8.76 (4H,m), δ 3.29-3.31 (4H,t, J=4.88Hz, 4.8Hz). ^{13}C NMR (100MHz, DMSO) 66.58, 66.83, 114.5, 115.3, 117.3, 117.9, 121.4, 122.9, 123.7, 126.6, 128.2, 128.2, 130.6, 136.8, 136.9.

Zinc, dichloride (4-(4-morpholinephenyl)-2,2':6',2"terpyridine) ($ZnCl_2L_2$). 4-(4-morpholinephenyl)-2,2':6',2" **L_2** (0.0947g, 0.24mmol) was dissolved in dichloromethane (12.3mL) in an Erlenmeyer flask. $ZnCl_2$ (0.0447g, 0.33mmol) in methanol (12.5mL) was slowly added to the Erlenmeyer and stirred for 3h. The solid was filtered and washed with methanol. The final solid yellow product had a less cotton like texture. Yield: 0.04309g, 33.8% ^{1}H NMR (400MHz, $CDCl_3$) δ 7.79-3.81 (4H,t, J=4.52Hz, 4.76Hz), δ7.17-7.19 (2H,d, J=8.68Hz), δ 7.86-7.88(2H,t, J= 6.00Hz, 5.64Hz), δ 8.25-8.35(4H,m), δ 8.82-8.83(2H,d, J=3.92Hz), δ 8.98-9.03 (3H,t, J=18.4Hz, 7.76Hz). ^{13}C NMR (100MHz, DMSO) 114.3, 117.9, 127.4, 129.8, 149.1.

4-(4-nitrophenyl)-2,2':6',2"terpyridine (L_3). 4-Nitrobenzaldehyde (1.0027g, 6.635mmol) and 2-acetylpyridine (1.620g, 1.08g/mL, 13.27mmol) were dissolved in methanol (60mL). An aqueous solution of KOH (5.25mL, 15%), and NH_4OH (56mL, 28-30%) were added and the reaction stirred vigorously for 3 days at room temperature. The crude product was filtered and rinsed with ethyl acetate resulting in a brown colored solid. The crude product was recrystallized in chloroform/hexane. The crude solid was dissolved in chloroform (63mL) and hexane was added until solution became cloudy. The solution was heated until the solution became clear, and the volume was reduced by half. The solution was hot filtered. The resulting precipitate was filtered and dried. The final product had a brownish clay color. Yield: 0.5683g, 24% ^{1}H NMR (400MHz, $CDCl_3$) δ 7.32 (2H,t, J=5.24Hz, 6.92Hz), δ 7.92 (2H,t, J=7.60Hz, 7.52Hz), δ8.06 (2H,d, J=8.52Hz), δ 8.31 (2H,d, J=7.92Hz), δ 8.689 (3H,t, J=6.20Hz, 4.64Hz). ^{13}C NMR (100MHz, DMSO) 124.3, 124.6, 128.5, 148.4.

Zinc, dichloride (4-(4-nitrophenyl)-2,2':6',2"terpyridine) ($ZnCl_2L_3$). 4-(4-nitrophenyl)-2,2':6',2" **L_3** (0.3977g, 1.122mmol) was dissolved in chloroform (5mL) in an Erlenmeyer flask. A solution of $ZnCl_2$ (0.01640g, 0.1203mmol) in methanol(3.97mL) was added to the Erlenmeyer and stirred for 3h. The resulting solid was filtered and washed with methanol. The final product was brown. Yield: 0.3120g, 56.7% ^{1}H NMR (400MHz, $CDCl_3$) δ 7.57 (2H,tt), δ 8.07 (2H,dd), δ 8.26 (2H,t, J=2.08Hz, 6.84Hz), δ 8.43 (2H,d, J=8.92Hz), δ 8.71 (2H,d, J=7.92Hz), δ 8.80 (3H,tt). ^{13}C NMR (100MHz, DMSO) 118.8, 121.5, 124.9, 125.2, 129.0, 138.1, 149.9, 155.1.

4-(4-aminophenyl)-2,2':6',2"terpyridine (L_4). 4-(4-nitrophenyl)-2,2':6',2" **L_3** (0.200g, 0.564mmol) was combined with $SnCl_2(H_2O)_2$ (0.789g, 3.5mmol) and HCl (5mL, 12M) in a round bottom flask. The reaction mixture was heated in an oil bath with stirring for 6h at 70°C. The mixture was cooled to room temperature and the solids vacuum filter and wash with water. The final product had light brown color. Yield: 0.1035 g, 56% ^{1}H NMR (400MHz, $CDCl_3$) δ 6.73-6.76 (2H,d, J=8.6Hz) δ 7.50-7.53 (2H,dd), δ 7.66-7.68 (2H,d, J=9.40Hz), δ 8.00-8.04 (2H,dd), δ 8.,63-8.67 (4H,m), δ 8.75-8.77 (2H,m). ^{13}C NMR (100MHz, DMSO) 114.7, 116.6, 121.3, 124.8, 128.1, 137.8, 149.7, 150.1, 155.8, 155.8.

Zinc, dichloride (4-(4-aminophenyl)-2,2':6',2"terpyridine) ($ZnCl_2L_4$). 4-(4-aminophenyl)-2,2':6',2" **L_4** (0.0993g, 0.31mmol) was dissolved in dichloromethane (13.2mL) in an Erlenmeyer flask. A solution of $ZnCl_2$ (0.0447g, 0.35mmol) in methanol (12.5mL) was added to the Erlenmeyer and stir for 3h. The precipitate was filtered and washed with methanol. The final product was a brownish orange color. Yield: 0.0862g, 61.1% ^{1}H NMR (400MHz, $CDCl_3$) δ 7.34-7.38 (2H,d, J=8.16Hz), δ 8.42 (2H,s), δ 8.65-8.67 (2H,d, J=7.96Hz), δ 8.86-8.90 (2H,t, J=7.56Hz, 7.16Hz), δ 9.38 (2H,s), δ 9.48-9.50 (4H,d, J=8.04). ^{13}C NMR (100MHz, DMSO) 114.7, 116.6, 121.3, 124.8, 128.1, 137.8, 149.7, 150.1, 151.0, 155.8, 155.8.

4-(4-hydroxyl)-2,2':6',2"terpyridine (L_5). 4-Hydroxybenzaldehyde (0.6101 g, 49.9mmol) and 2-acetylpyridine (1.21g, 1.08g/mL, 9.988 mmol) were combined in ethanol (25mL). NaOH pellets (2.0559g) were added and the solution was stirred vigorously until pellets dissolved completely. NH_4OH (8mL, 28-30%) was added to the reaction mixture and stirred at room temperature for 24 h. The pale white precipitate was filter and wash with ethanol and water. The crude product was filtered from ethanol resulting in a dule pale white crystalline product. Yield: 1.145g, 70.31% ^{1}H NMR (400MHz, $CDCl_3$) δ 7.04-7.06 (2H,d, J=8.68Hz) δ 7.9-7.95 (2H,t, J=6.68Hz, 6.04Hz) δ 7.97-8.05 (2H,d, J=8.68Hz) δ 8.40-8.52 (2H,m) δ 8.87-8.91 (2H,s), δ 8.94-8.97 (2H,d, J=4.36Hz), δ 9.02-9.09 (2H,d, J=8.08Hz)

CHAPTER 3: RESULTS AND DISCUSSION

3.1 RESEARCH PLAN

This project is aimed at improving current organozinc complexes (1a-c) found in the literature, which act as indicators for pyrophosphate (**PPi**) anion[1,2] (**Figure 9**). The first phase of the project was to repeat literature procedures to validate our methods before applying them to new molecules. This phase employs zinc dichloride (4-(4-dimethylaminophenyl)-2,2':6',2" terpyridine) (**$ZnCl_2L_1$**) to validate the method and ensure the reliability of the techniques described in the literature, namely fluorescence spectrum and Job's plot. The project's second phase involved synthesizing new zinc dichloride terpyridine (**$ZnCl_2L$**) complexes and testing their ability to act as fluorescent indicators for **PPi** anions. The third phase of the project was evaluating the use of the **$ZnCl_2L$** complexes in applications such as confocal microscopes.

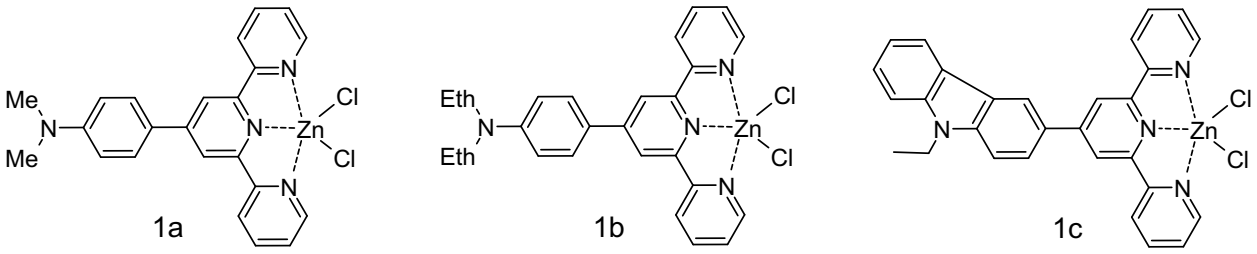

$ZnCl_2L_1$

Figure 9. Structures of 1a) zinc dichloride (4-(4-dimethylyaminophenyl) 2,2':6',2"terpyrdine, 1b) zinc dichloride (4-(4-diethylyaminophenyl) 2,2':6',2"terpyrdine, and 1c).

3.2 METHOD VALIDATION

The reported **$ZnCl_2L$** complexes were also shown to have high selectivity and sensitivity for **PPi** anion. The **$ZnCl_2L$** complexes (1a-c) reported in the literature were shown to coordinate in a 3:1 ratio with the **PPi** anion. This was verified by performing fluorescence titration to produce a fluorescence spectrum and a Job's method. The spectrum of the titration study shows the change in fluorescence intensities at different molar fractions. A Job's plot is a method of determining stoichiometry by continuous variation, where the concentration of a product is measured after varying the mole fractions of the reactants. The stoichiometry is determined by plotting the product concentration verse the mole fraction. The maximum on concentration of the plot gives the mole fraction at the stoichiometric equivalence point. In this study, fluorescence intensity, which is proportional to nano-aggregate concentration, was plotted against mole fraction of **PPi**. The **$ZnCl_2L_1$** was selected to validate our methods before testing new ligands and their zinc complexes. Many difficulties arose in attempting to repeat the literature procedure.

3.2.1 SYNTHESIS OF $ZnCl_2L_1$

The synthesis of **$ZnCl_2L_1$** (1a) was straightforward and proceeded in good yield. The synthesis of the 4-(4-dimethylyaminophenyl)-2,2':6',2"terpyrdine (**L_1**) involved reacting p-dimethylaminobenzaldehyde, 2-acetylpyridine, and KOH in aqueous ammonium hydroxide.

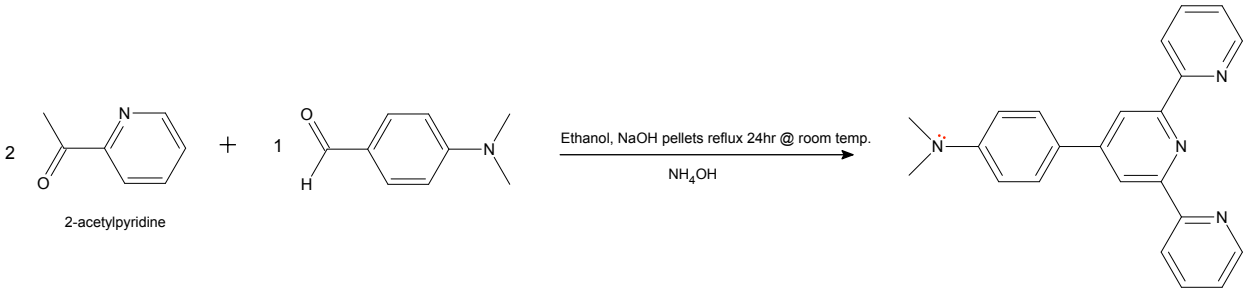

Scheme 2. Synthesis of 4-(4-dimethylyaminophenyl)-2,2':6',2"terpyrdine (**L_1**).

The **L_1** , dissolved in CH_2Cl_2 was combined with an ethanol solution containing $ZnCl_2$ to from the **$ZnCl_2L_1$** complex.

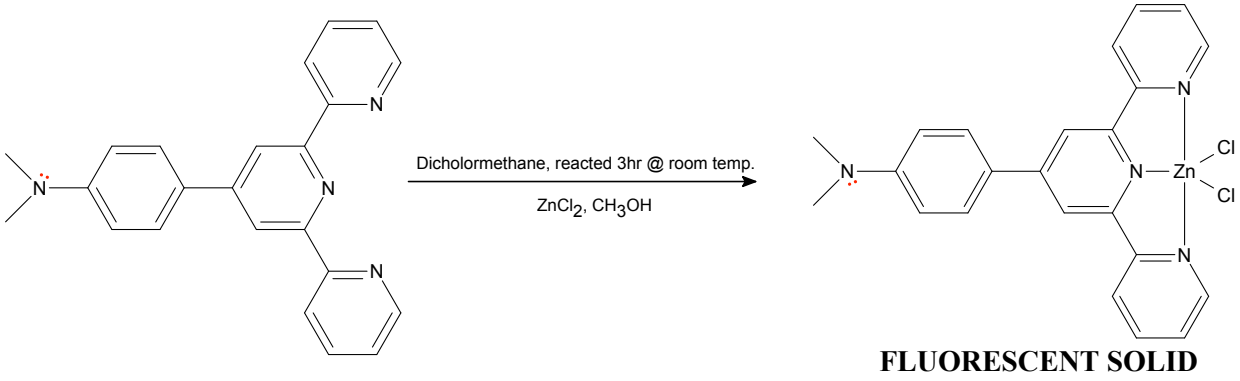

Scheme 3. Synthesis of zinc, dichloride 4-(4-dimethylyaminophenyl)-2,2':6',2"terpyrdine **($ZnCl_2L_1$)**.

*3.2.2 Fluorescence Titration and Jobs Plot for **$ZnCl_2L_1$***

Difficulties occurred in repeating the reported fluorescence titration and Job's method for **$ZnCl_2L_1$**. It was clear that many critical experimental details were omitted in the published literature. Inconsistent data was obtained throughout the **PPi** titration study. When running the plates in the SpectraMax iD5 multimode microplate reader, using fluorescence spectrum mode, the data varied each time or day. Possible sources of error were instrument error, human error, or issues with the compounds being measured.

To rule out instrument and human error, a fluorescence titration was performed on quinine standards. The SpectraMax iD5 multimode microplate reader was the source of inconsistent data issues, which were addressed by creating a standardized solution of 0.1 ppm quinine, diluted with nano-pure water, to serve as a standard curve for instrument calibration before each use. The results from the quinine titration revealed a linear plot of fluorescence intensity versus concentration and ruled out user and instrument error.

Issues were discovered with the **PPi** anion and **$ZnCl_2L$** complex, which deteriorated over time, producing unreliable data from the SpectraMax iD5 multimode microplate reader. It was found that fluorescence titrations run using older stock solutions of **PPi** produced results that did not match previous measurements. **PPi** anions in solution are unstable and can hydrolyze to form inorganic phosphate (HPO_4^{2-}). As a result, the concentration of our **PPi** stock solutions changed over time leading to inconsistent results. Additionally, HPO_4^{2-} can bind with the **$ZnCl_2L$** complex and result in a decrease in fluorescence. To verify the selectivity of **$ZnCl_2L$** for recognizing **PPi**, interactions between **$ZnCl_2L$** and various other anions were studied in **Figure 2**. The researchers used absorption measurements to show that other phosphate anions do not cause spectral changes similar to those caused by **PPi**, thereby highlighting the specific binding interactions between **$ZnCl_2L$** complexes and **PPi. Figure 10** illustrates multiple anions that can be present in DNA, and it reveals that the **$ZnCl_2L$** complex has a higher absorbance when binding to **PPi.**

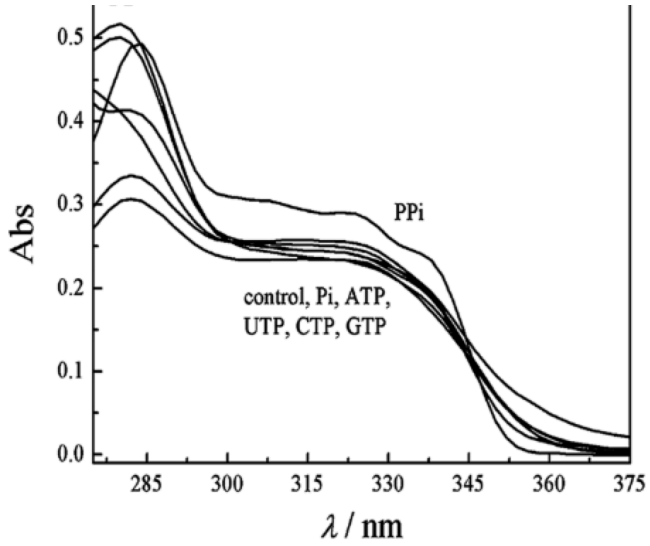

Figure 10. Absorption spectra of **$ZnCl_2L$** complex in the absence and presence of various phosphates[5].

An additional complication involved the stability of the **$ZnCl_2L_1$** complexes. The reproducibility of measurements made on **$ZnCl_2L_1$** varied over several days. The **$ZnCl_2L_1$** appears to degrade over time. One possibility is that **$ZnCl_2L_1$** in solution undergoes photobleaching. Another possibility is that the **$ZnCl_2L_1$** dissociates into $ZnCl_2$ and **L_1** when diluted to low concentration. We prepared 100 μM solutions and stored ZnCl2L complexes in the dark to prevent photobleaching. The solid forms of the terpyridine (**L**) and **$ZnCl_2L$** (as described in the Experimental section SOP) complexes were utilized solely for characterization purposes, since they degraded early in the project.

Despite taking these precautions, the reproducibility issue persisted, so we opted for an alternative method in our fluorescence titration study. Daily, the **$ZnCl_2L_1$** complex was freshly prepared in solution prior to running the study. By combining a solution of $ZnCl_2$ and **L_1** in a HEPES buffer (as described in the Experimental section). Another possible problem is that the 3:1 **$ZnCl_2L$:PPi** complex may not have aggregated to form the fluorescent nanoaggregates.

Altering the p-substituent can change the complexes water solubility can impact the aggregated formation. The **$ZnCl_2L_1$** complex's ability to aggregate, which is necessary for a fluorescence response, may be influenced by its solubility, as well as the size, shape, and presence of lone pairs on the R-group.

In conclusion, the **$ZnCl_2L_1$** complex in solution and solid form can deteriorate and experience photobleaching, which causes the fluorescence properties of the aggregates to decrease over time. After resolving these difficulties, we successfully repeated the fluorescence titration and Jobs plot for **$ZnCl_2L_1$** and all other **$ZnCl_2L$** complexes. **(Scheme 3).**

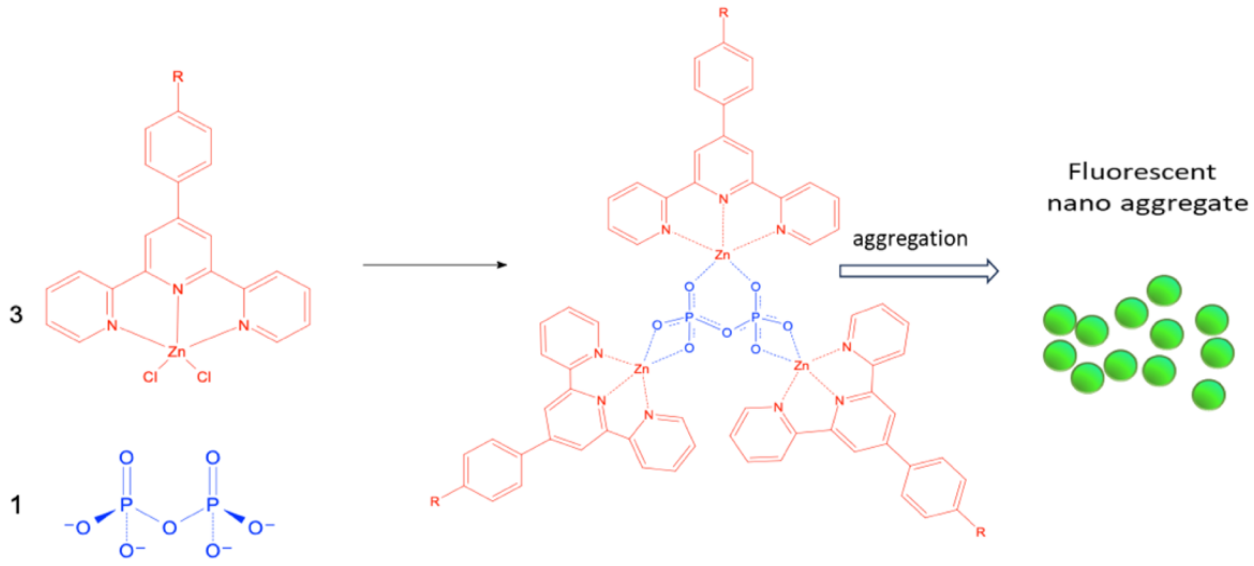

Scheme 4 Formation of a 3:1 **PPi- $ZnCl_2L$** complex and formation of a fluorescent nano-aggregate.

For the titration study, a series of stock solutions of **L_{1-4}**, zinc dichloride ($ZnCl_2$), and **PPi** anion is made up in HEPES buffer (pH 7.4). To make up the 100 µM **$ZnCl_2L$** complex solution, a mixture of 100 µL $ZnCl_2$ (25 mM) dissolved in methanol and 2 mL **L** (2.5 mM) dissolved in methanol was combined in a 50 mL volumetric flask, and then diluted with 50 mL HEPES buffer

(pH 7.4) and sonicated for 5 minutes. By varying the volumes, we obtained different molar fractions for the **PPi** anion, revealing an unusual 1:3 binding stoichiometry (Table 1 in SI), which is supported by the Jobs method plot and fluorescence spectra. The titration plot of 100 µM **$ZnCl_2L_1$** adding 100 µM **PPi** shows an emission of 591 nm. The highest curve in **(Figure 11a**) shows the binding stoichiometry of the 3:1 ratio of **$ZnCl_2L_1$** and **PPi** anion. Another confirmatory test, known as a Job Plot, proves the stoichiometric relationship between **$ZnCl_2L_1$** and the **PPi** anion (**Figure 11b**.). The yellow dotted line serves as an indicator of the 3:1 ratio and also compares the intensity of fluorescence to all other data points.

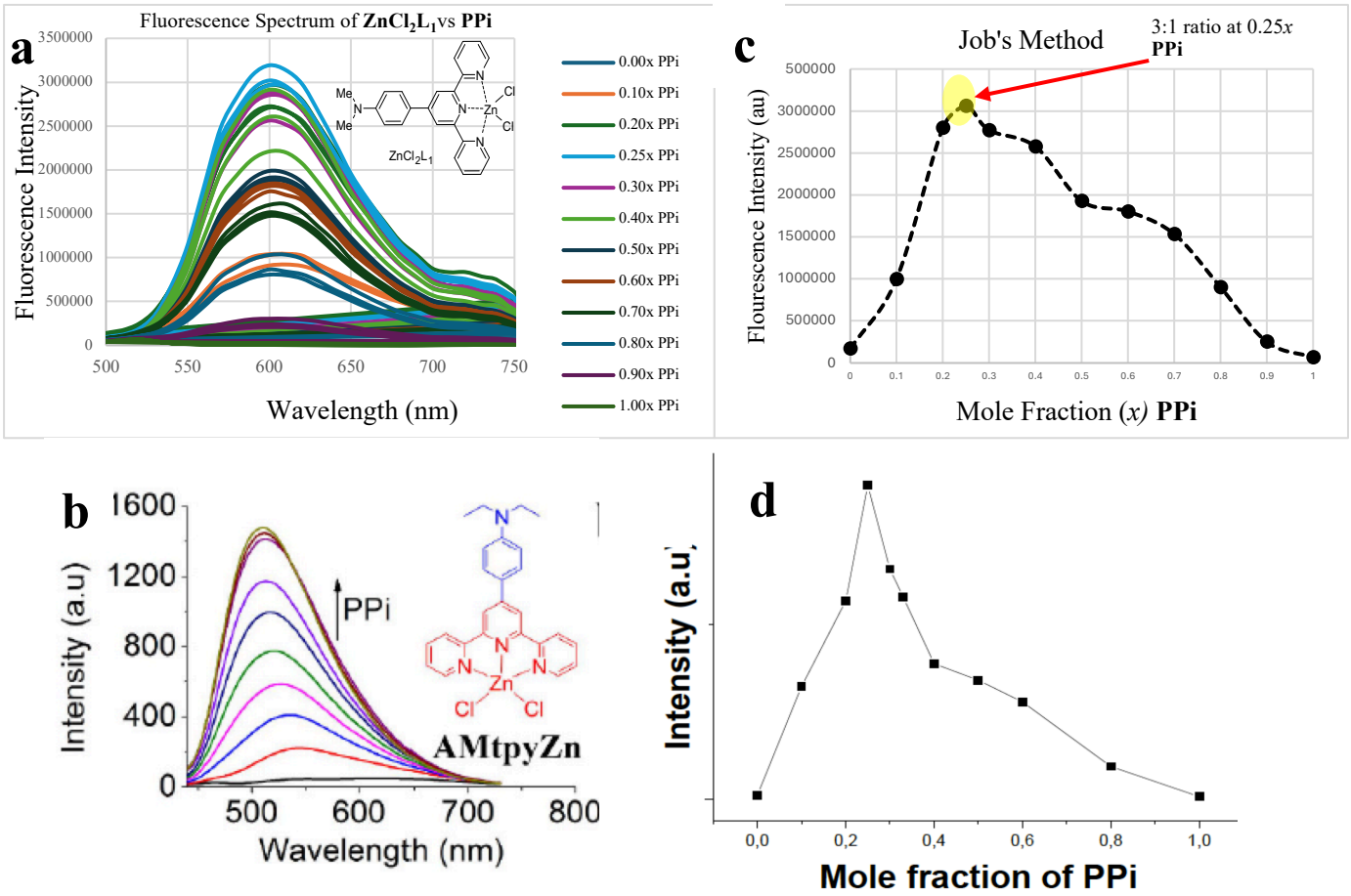

Figure 11. a) Fluorescence titration of **$ZnCl_2L_1$**(100uM) with **PPi** (100uM) at varying volumes in replication of 3 [excitation 440nm and emission 591nm] .**b)**literature [2] results: fluorescence titration **$ZnCl_2L_1$**(10uM) with **PPi** (10uM). **c)** Job's method **d)** Job's method analysis of our results and the literature showing a 3:1 **$ZnCl_2L_1$:PPi** ratio.

We were able to successfully reproduce the literature[2] results with $\mathbf{ZnCl_2L_1}$ demonstrating the formation of a 3:1 **PPi-** $\mathbf{ZnCl_2L_1}$ complex and formation of a fluorescent nano-aggregate (**Scheme 4.**).

3.3 NEWLY SYNTHESIZED TERPYRIDINE AND ZINC, DICHLORIDE-TERPYRIDINE COMPLEXES

3.3.1 SYNTHESIS OF L_2, L_3, *AND* L_4

The newly synthesized **L** complexes differed only in the presence of an R-group. Most compounds were prepared by dissolving R-benzaldehyde and 2-acetylpyridine in ethanol, following a general procedure. Then NaOH/KOH pellets were added to the solution with vigorous stirring until the pellets dissolved completely. Concentrated NH_4OH (28-30%) was added and the reaction was stirred at room temperature for 16 h. The precipitate was filtered and washed with ethanol/methanol, which is shown in **Schemes 4** and **5.**

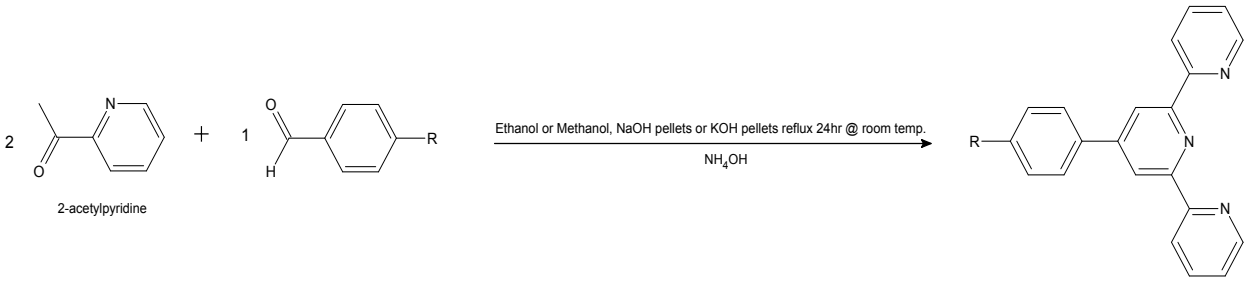

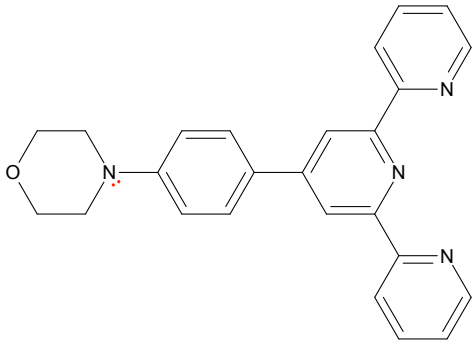

L_2.

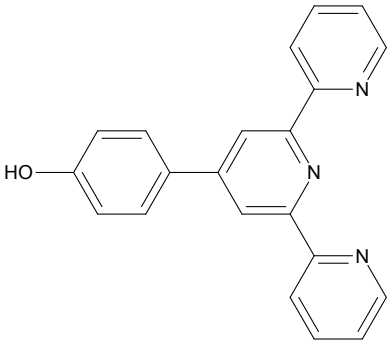

L_5

Scheme 5. Synthesis of 4-(4-morpholinephenyl)-2,2':6',2"terpyridine **(L_2) and 4-(4-hydroxyl)-2,2':6',2"terpyridine (L_5).**

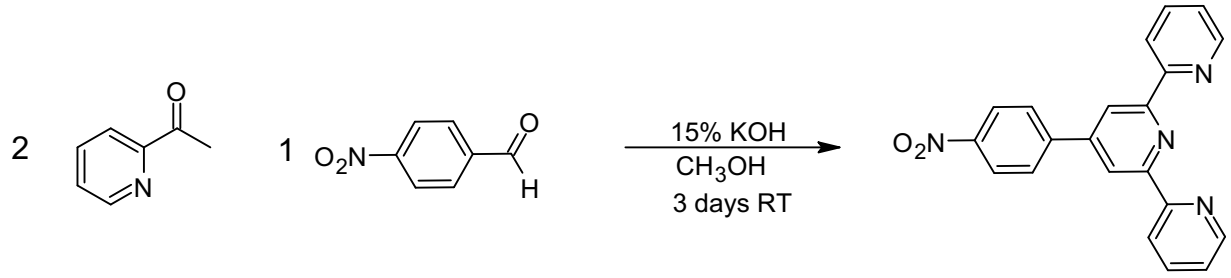

Scheme 6. Synthesis of 4-(4-nitrophenyl)-2,2':6',2"terpyridine (**L_3**).

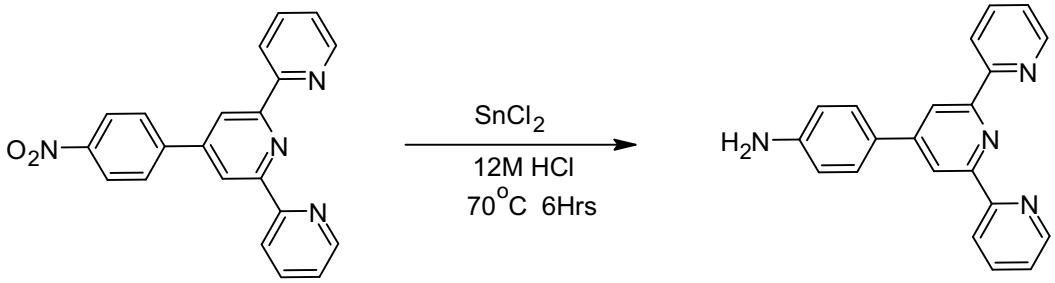

Scheme 7. Synthesis of 4-(4-aminophenyl)-2,2':6',2"terpyridine **(L_4).**

3.3.2 SYNTHESIS OF $ZnCl_2L_2$, $ZnCl_2L_3$, *AND* $ZnCl_2L_4$

In the newly synthesized **$ZnCl_2L$** complexes, a general procedure was meticulously followed, where **L** was carefully dissolved in a mixture of dichloromethane or chloroform, and $ZnCl_2$ was separately dissolved in methanol. Then, the reaction mixture was stirred at room temperature for a period of three hours. Subsequently, the resulting precipitate was filtered and thoroughly washed with a solvent mixture of ethanol and methanol, as illustrated in **Scheme 7**.

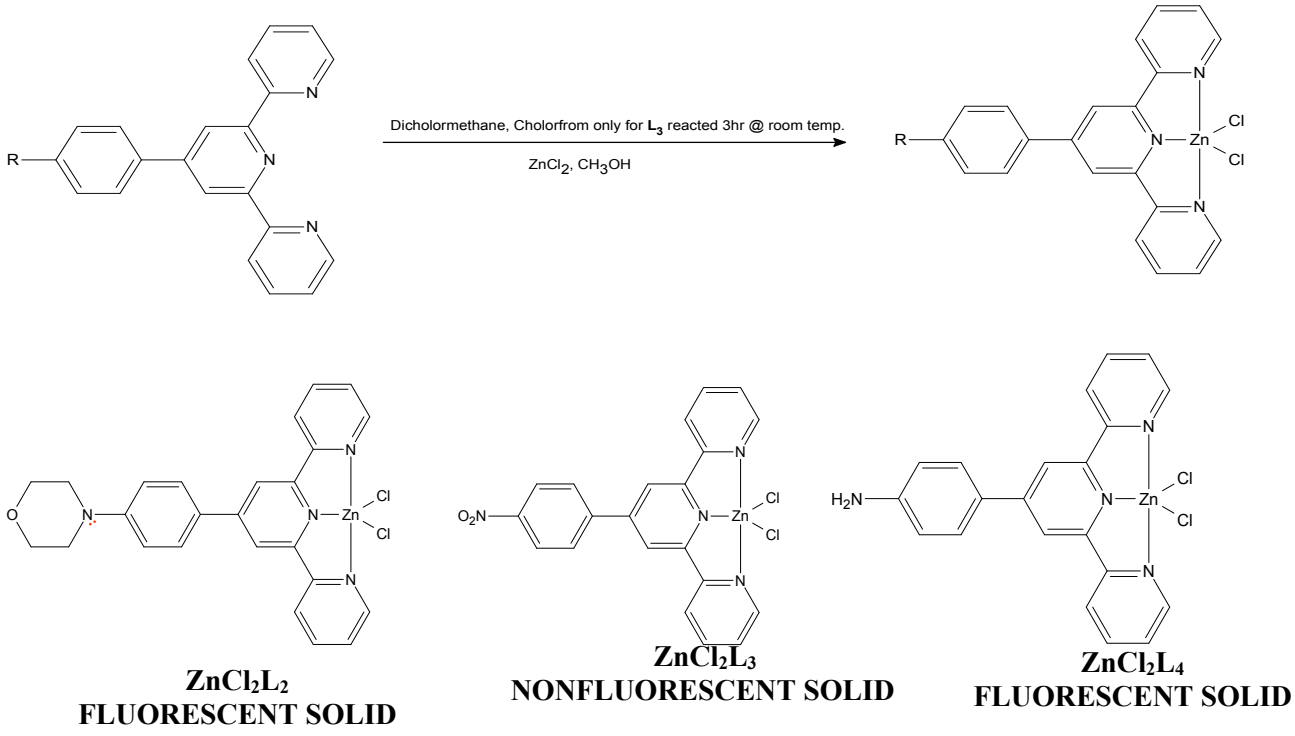

Scheme 8. Synthesis of Zinc, dichloride (4-(4-morpholinephenyl)-2,2':6',2"terpyridine) (**$ZnCl_2L_2$**), Zinc, dichloride (4-(4-nitrophenyl)-2,2':6',2"terpyridine) (**$ZnCl_2L_3$**), and Zinc, dichloride (4-(4-aminophenyl)-2,2':6',2"terpyridine) (**$ZnCl_2L_4$**).

*3.3.3 $ZnCl_2L_{2\text{-}4}$ COMPLEXES **PPi** TITRATION STUDIES*

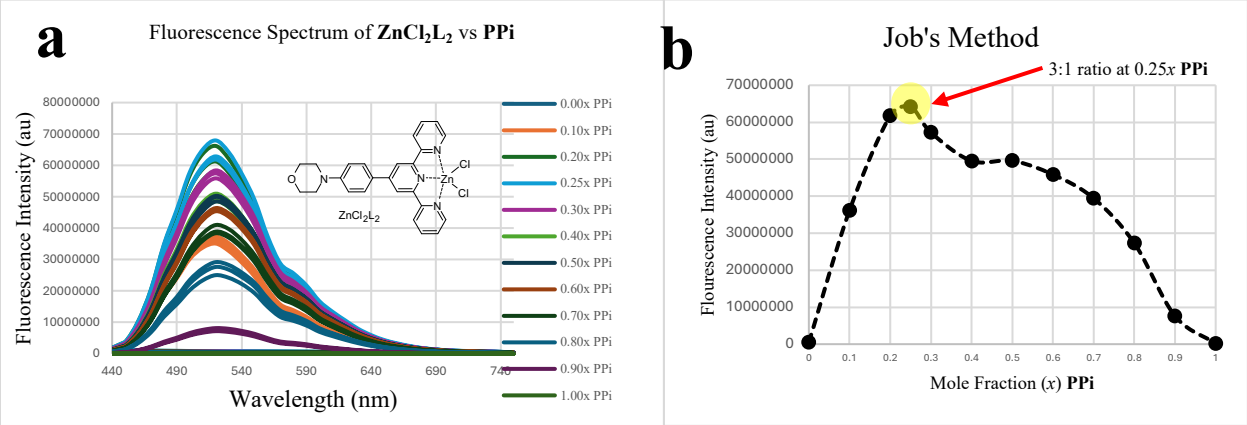

Figure 12. a) Fluorescence spectrum of **$ZnCl_2L_2$** (100uM) [excitation 400nm and emissions 520nm] upon addition of **PPi** (100uM) in replication of 3 b) A Job Plot analysis for **PPi** binding to **$ZnCl_2L_2$.**

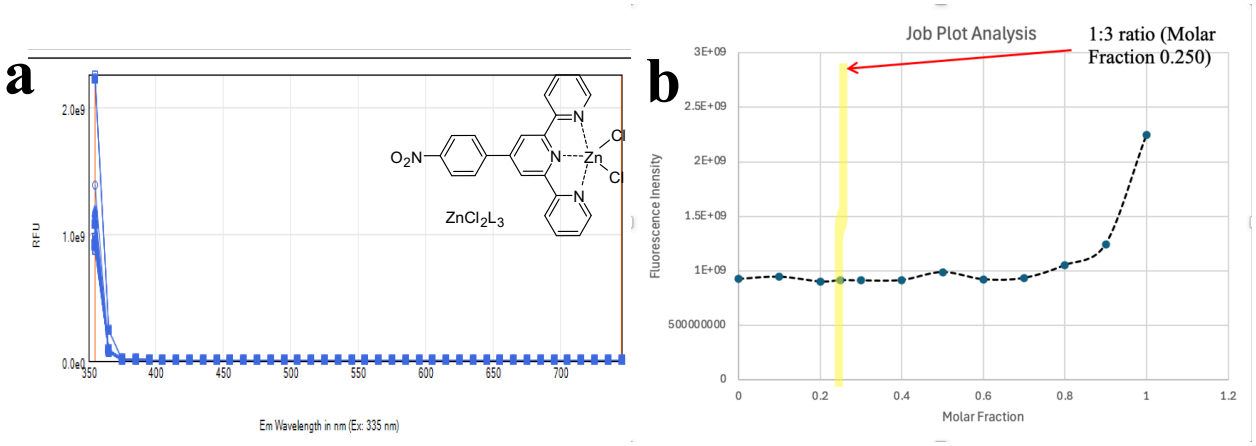

Figure 13. a) Fluorescence spectra of **$ZnCl_2L_3$** (100uM) [excitation 335nm and emissions 355nm] upon addition of **PPi** (100uM) in replication of 3 **b)** A Job Plot analysis for **PPi** binding to **$ZnCl_2L_3$**.

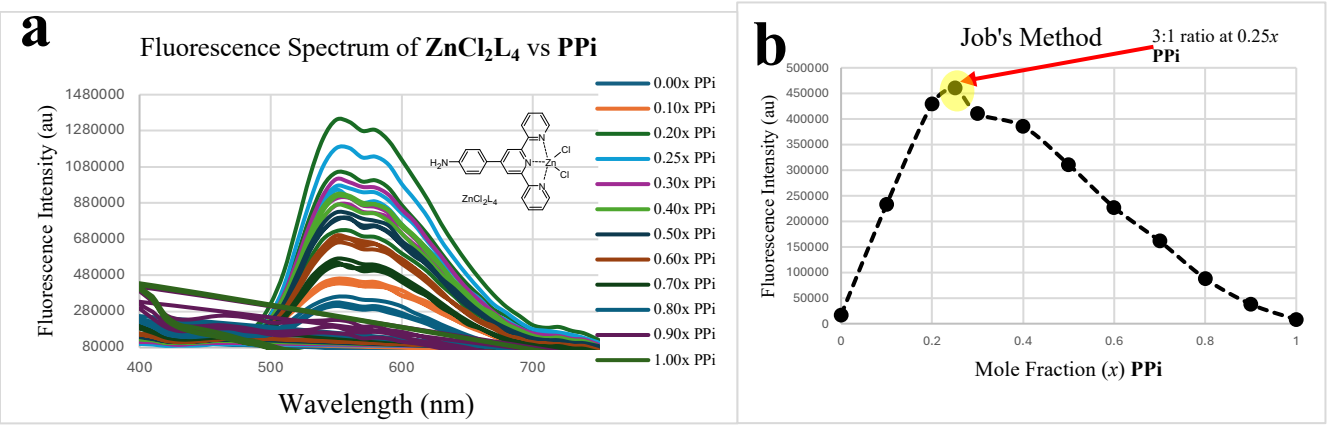

Figure 14. a) Fluorescence spectrum of **$ZnCl_2L_4$** (100uM) [excitation 350nm and emissions 570nm] upon addition of **PPi** (100uM) in replication of 3 **b)** A Job Plot analysis for **PPi** anion binding to **$ZnCl_2L_4$** at a 1:3 ratio.

Fluorescence titration and Job's plot data were collected for **$ZnCl_2L_{(2\text{-}4)}$**. All the ligands, specifically those with a para-amino group, such as **L_2** and **L_4**, fluoresced brightly when in the presence of **PPi**. Additionally, the Job's plot of **$ZnCl_2L_2$** (**Figure 12b**) and **$ZnCl_2L_4$** (**Figure 14b**) showed the expected 3:1 stoichiometry, thereby demonstrating that they form fluorescent nanoaggregates by the same mechanism as **$ZnCl_2L_1$**, as depicted in **Figure 12b** and **d.** The **$ZnCl_2L_3$** complex, characterized by its para-NO_2 functional group, failed to exhibit any fluorescence properties during the titration study, as depicted in **Figure 13.** We were unable to determine whether the **$ZnCl_2L_3$** is forming a 3:1 complex using this particular method.

In the ground state, the zinc complex adopts the geometry as shown in 1a–ZnX_2, in which the phenyl "A" is not coplanar with the terpyridine plane (twisted by about 40°, based on a literature modeling study)[3]. Intramolecular charge transfer (ICT) interaction occurs when an excited molecule (R-group) acts as a donor and the neighboring molecule (**$ZnCl_2L$**) acts as an acceptor (**Figure 15a**). In the excited state, the two aromatic rings A and B will become coplanar, which leads to increased donor–acceptor interaction. The donor-acceptor interaction

must be capable of producing both a locally excited state and a TCIT state. TICT is one of the photophysical phenomena that occur in fluorescent molecules as a result of photoexcitation. After twisting, the molecule returns to the ground state from the TICT state by emitting radiation in a longer wavelength region or through nonradiative decay.

The locally excited state is a physical system in which excitation is localized due to the lone pairs, requiring a stronger electron for zinc-induced fluorescence quenching, since without the lone pairs, the nitrogen can rotate away from its coplanarity with phenyl, leading to a twist intramolecular charge transfer (TICT). The electron-donating NMe_2 substituent thus enabled a strong donor–acceptor interaction in the 1a–Zn complex while the donor group was turned in a coplanar position with the phenyl group (**Figure 15b**)[3]. **Figure 7c** shows how the charge from the R-group and the **$ZnCl_2L$** are distributed across the molecule, causing a slight positive charge on the R-group and a slight negative charge on the **$ZnCl_2L$** complex.

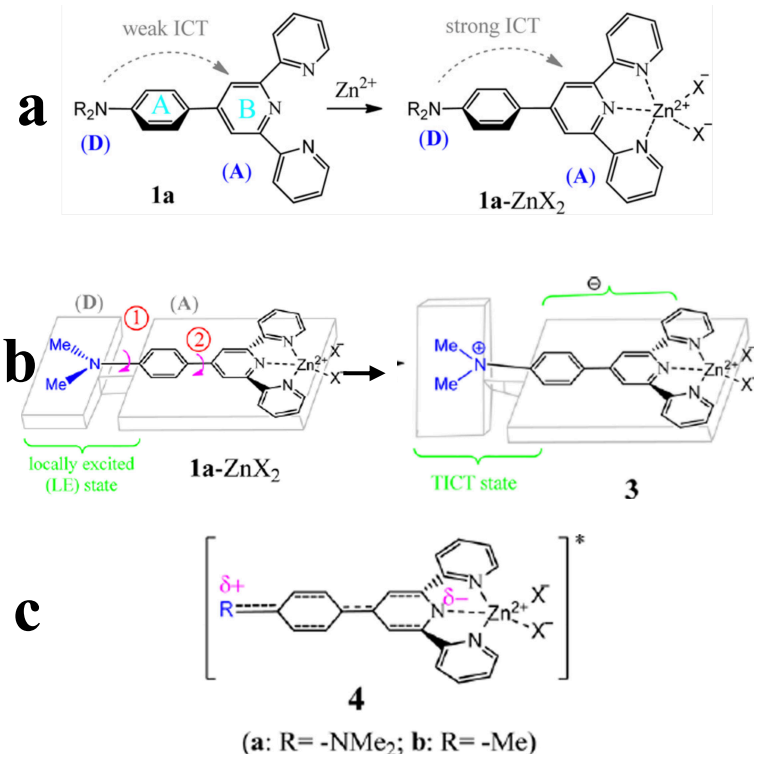

Figure 15. Scheme of a) Showing how the ICT interaction between terpyridine (1a) is weaker compared to **$ZnCl_2L$,** b) illustrate LE and TICT state by rotating of the amine group and, c)how the charges of the electrons are distributed in the **$ZnCl_2L$** complex[6].

Comparison of the titration results showed that the **$ZnCl_2L_2$** had improved fluorescence intensity over the **$ZnCl_2L_1$** reported in the literature(**Graph 1**). The maximum intensities for **$ZnCl_2L$** complexes at the molar fraction0.25 are **$ZnCl_2L_1$** (3,059,619.333 au.), **$ZnCl_2L_2$** (64,222,337.33 au.), and **$ZnCl_2L_4$** (460,131 au.). The **$ZnCl_2L_2$** also had greater water solubility than **$ZnCl_2L_1$**. The higher fluorescence intensity and water solubility should make **$ZnCl_2L_2$** a better tool in assays for **PPi** and dye for staining nuclei in confocal microscopy.

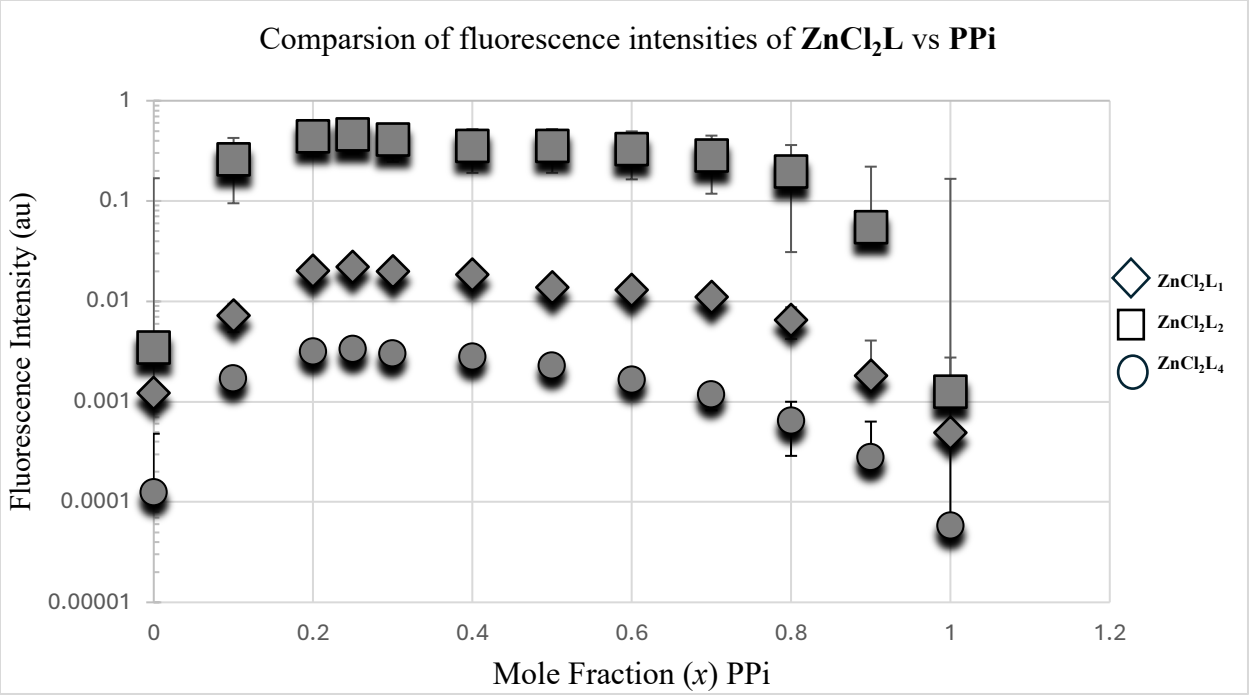

Graph 1. Comparison of fluorescence intensities vs **PPi** of **$ZnCl_2L_1$, $ZnCl_2L_2$, and $ZnCl_2L_4$** at logarithmic scale**.**

3.4 CONFOCAL MICROSCOPE BIOIMAGING

We further researched the capability of **$ZnCl_2L_1$** and **$ZnCl_2L_2$** in cell imaging. The **$ZnCl_2L_2$** complex containing the morphyl group exhibits a higher intensity, as shown in **Graph 1** compared to **$ZnCl_2L_1$**. We wanted to evaluate the use of the two complexes in confocal microscope imaging. The **$ZnCl_2L_4$** was not used in the confocal microscope's imaging due to its low fluorescence intensity compared to the other complexes (**Graph 1**). The **$ZnCl_2L_1$** was prepared by dissolving the solid in a mixture of 1% DMSO and nanopure H_2O, due to its low solubility in water. In contrast, the **$ZnCl_2L_2$** was prepared by dissolving the solid in nanopure H_2O, given its high solubility in water.

There were about three or four different images that were recorded. Brightfield is used to see the wide range of the cells. The fluorescence field is used to visualize the $ZnCl_2$ binding to **PPi**, which stains the cell nucleus. The Hoechst stain is a general dye stain for DNA due to its lower toxicity compared to DAPI. The Hoechst stain binds to the minor groove of double-stranded DNA, and the Hoechst dyes can bind to the DNA in live or fixed cells. [6]

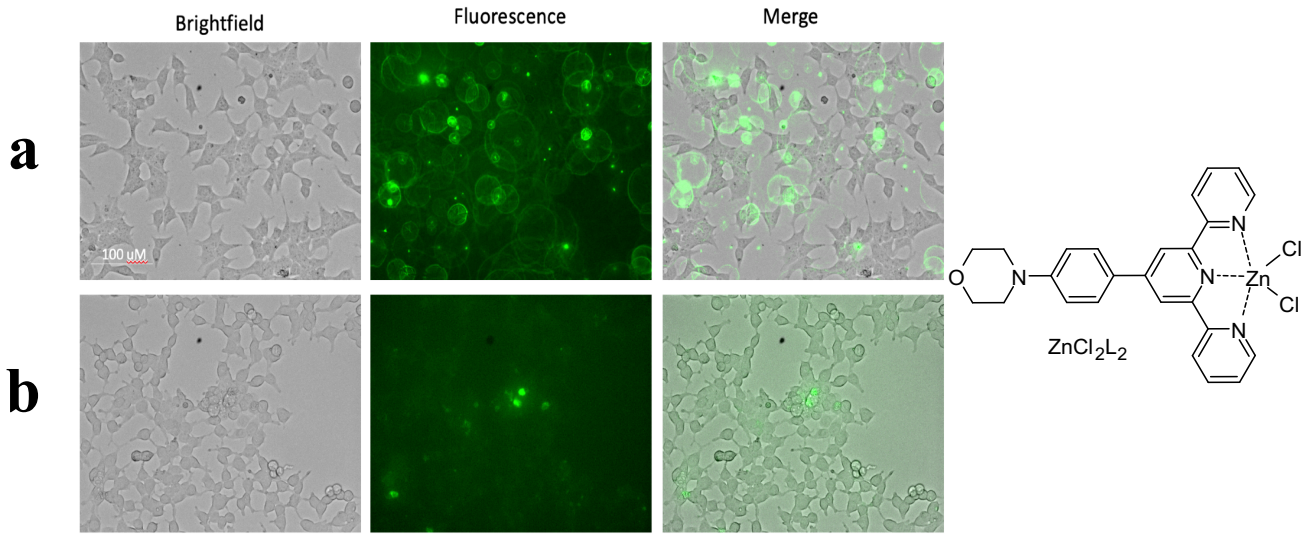

Figure 16. Confocal fluorescence microscope images of 10uM **$ZnCl_2L_2$** incubated in **a)** DMEM for 30mins **b)** HEPES buffer pH 7.4 for 30 mins.

The **$ZnCl_2L_2$** was added to HEK293 cells that are grown in growth media DMEM, which is a basal medium that supports the growth of many different mammalian cells. The cells were then washed with a 10 mM HEPES image buffer solution, pH 7.4, comprising 125 mM NaCl, 5 mM KCl, 1.2 mM $MgCl_2$, 1.3 mM $CaCl_2$, 25 mM HEPES, 3 mM D-glucose, and NaOH (adjusted to pH 7.4), and brought to a total volume of 250 mL with ddH_2O[4]. Following this, the cells were treated with a 10 µM $ZnCl_2$ solution for 30 minutes at room temperature, incubated

for 30 minutes, and images were recorded in **Figure 16**. The **$ZnCl_2L_2$** complex in **Figure 16a** shows a lot of aggregation outside the cell and little aggregation inside the cell. In **Figure 16b** the HEPES buffer appears to show little aggregation inside the cells. The results shown in **Figure 16** could have been due to a low concentration of the **$ZnCl_2L_2$**, or the **$ZnCl_2L_2$** may have issues crossing the cell membrane to bind to **PPi**.

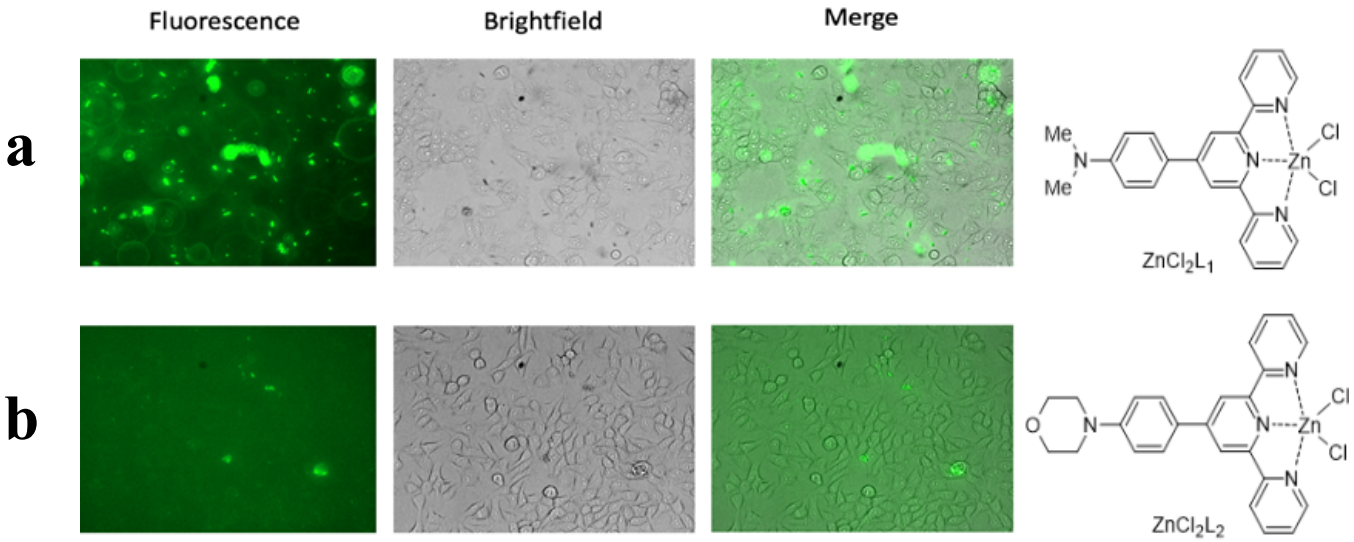

Figure 17. Confocal fluorescence microscope images **a)** 200uM **$ZnCl_2L_1$** **b)** 200uM **$ZnCl_2L_2$** added to HEK293 cells for 30mins in imaging buffer.

HEK293 cells were grown in a medium containing both **$ZnCl_2L_1$** and **$ZnCl_2L_2$**, washed with a 10mM HEPES image buffer solution (pH 7.4), then treated with a 200uM **$ZnCl_2L$** solution for 30 minutes at room temperature; afterwards, images were recorded. The incubation time was only 30 minutes for both complexes, and it seems that **$ZnCl_2L_1$** was able to cross the cell membrane of the cells faster (**Figure 17a**). Unlike **$ZnCl_2L_2$**, which shows little complex crossing the cell membrane, as shown in **Figure 17b**. The **$ZnCl_2L_1$** aggregates more easily than the **$ZnCl_2L_2$**. Even though **$ZnCl_2L_2$** is more water soluble, its higher water solubility might

cause it to have poor lipophilicity. It makes it particularly difficult for **$ZnCl_2L_2$** to pass through the cell membrane, which is selectively permeable. However, the **$ZnCl_2L_1$** (**Figure 17a**) stained more nuclei than the **$ZnCl_2L_2$** (**Figure 17b**). We assume this is due to differences in the two complexes' ability to cross the cell membrane.

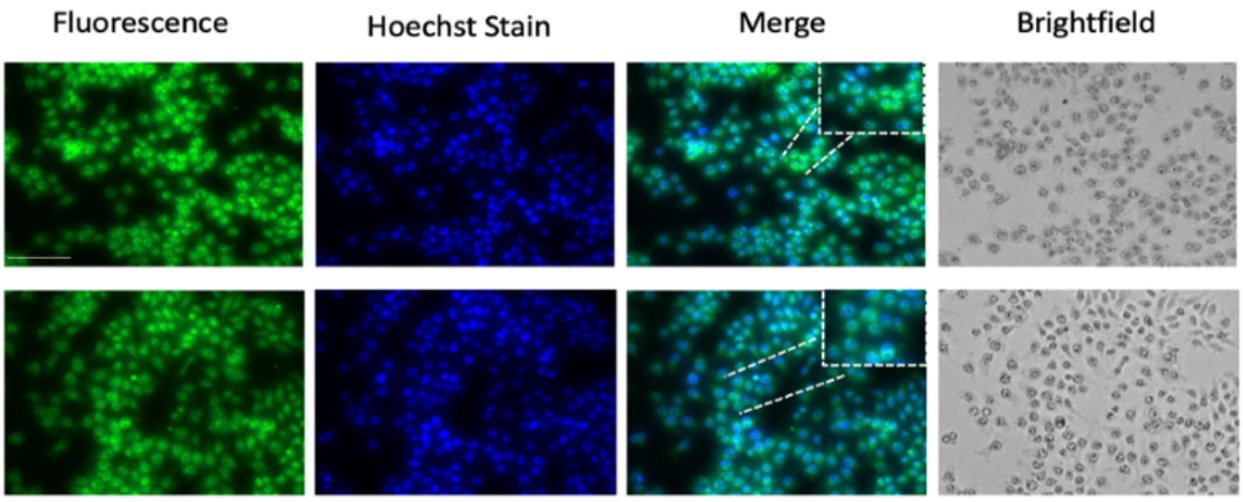

Figure 18. Confocal fluorescence microscope images **a)** 200uM **$ZnCl_2L_1$** 4-(4-dimethylaminophenyl)-2,2':6',2". **b)** 200uM **$ZnCl_2L_2$** 4-(4-morpholinephenyl)-2,2':6',2" added to HEK293 cells for 24 hrs. in imaging buffer.

The HEK293 cells were then stained with Hoechst stain, **$ZnCl_2L_1$**, and **$ZnCl_2L_2$** to demonstrate that **$ZnCl_2L$** complexes were staining the nuclei of the cells. The HEK293 cells were incubated with **$ZnCl_2L_1$** and **$ZnCl_2L_2$** for 24 hours to allow sufficient time for the nuclei to stain and for **$ZnCl_2L_2$** to diffuse across the cell membrane and into the nuclei. An overlay of images for Hoechst stain, **$ZnCl_2L_1$** (**Figure 18a**), and **$ZnCl_2L_2$** (**Figure 18b**) clearly shows that they stain the same areas of the cell (**Figure 19a**). This is expected since the nucleus has high concentration of **PPi** anions.

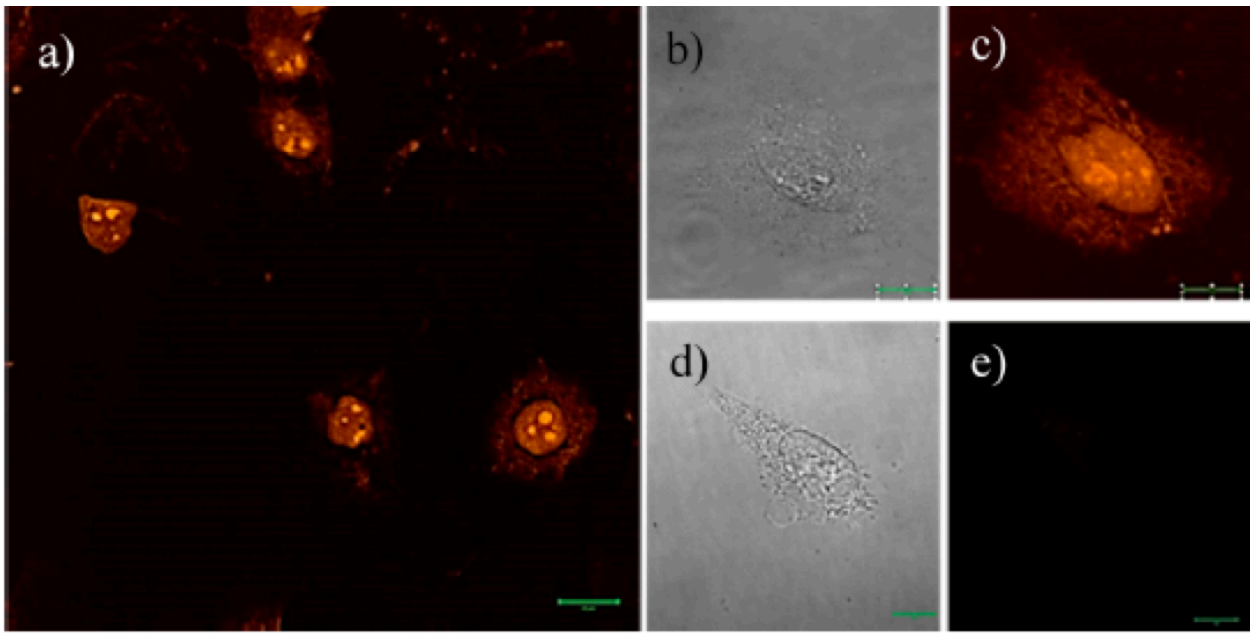

Figure 19 Confocal fluorescence microscopy images of **a)** HeLa cells incubated with probe **$ZnCl_2L_1$** (50 μM), **c)** single HeLa cell, and **e)** single HeLa cell without staining (control). Differential interference contrast images of **b)** single HeLa cell incubated with probe **$ZnCl_2L_1$** (50 μM) and **d)** single HeLa cell without staining (control)**Error! Bookmark not defined.**.

In the article '*A Fluorescent Pyrophosphate Sensor with High Selectivity over ATP in Water*[1],' HeLa cells were grown in DMEM (containing 10% fetal bovine serum and antibiotics) for 16 hours. They washed their cells with 10 mM HEPES buffer, pH 7.4, containing 137 mM NaCl, then treated them with 10 μM **$ZnCl_2L_1$** for 30 min in the same buffer at 37 °C, and washed extensively with buffer before imaging. They recorded the data after laser excitation at 488 nm, using emission wavelengths between 555 and 655 nm to detect orange-red fluorescence.

In the images, they said that the bright orange- yellow parts are where the **$ZnCl_2L_1$** binds to **PPi** in the HeLa cells. Referring to **Figure 19** and my own **Figure 18**, it appears that **$ZnCl_2L_1$**

This is shown in **Figure 18a** for **$ZnCl_2L_1$** and **Figure 18b** for **$ZnCl_2L_2$**. It is clear that the **$ZnCl_2L_{1-2}$** complexes bind to **PPi** and stain the HEK293 cells

2.5 DISCUSSION

In conclusion, our study demonstrates that the zinc dichloride 4-(4-morpholinephenyl)-2,2':6',2" terpyridine (**$ZnCl_2L_2$**) complex exhibits a higher fluorescence response to **PPi** and better water solubility compared to the previously recorded zinc dichloride 4-(4-dimethylaminophenyl)-2,2':6',2" terpyridine (**$ZnCl_2L_1$**). Both **$ZnCl_2L_{1-2}$** complexes show a fluorescence response and great selectivity to the **PPi** anion. The **$ZnCl_2L_{1-2}$** complexes successfully stain the HEK293 cells for fluorescence imaging. By showing how sensitive these complexes are, we hope that they will potentially be useful indicators of metabolic function like ATP hydrolysis and diseases such as calcium pyrophosphate dihydrate crystal deposition disease. These complexes could be used to better understand DNA synthesis and any problems related to mutations in the genetic code, cell death, and cancer development. The next stage of this research would involve using **$ZnCl_2L_{1,2, \text{ and } 3}$** complexes in a DNA Polymerase bioassay to examine how effectively they bind to the **PPi** anion in real-time as it is formed.

Other future research could involve finding more water-soluble selective and sensitive probes for **PPi** detection. These molecules can allow researchers to monitor **PPi** concentration in various cellular processes. The binding of **PPi** to a **$ZnCl_2L$** complex can be detected by changes in fluorescence intensity, which is related to enzyme activity, bone mineralization, and metabolism. This information could be very favorable to other areas of study, like cancer, where abnormal **PPi** levels can be indicative of disease progression. A more popular area of study is

drug discovery, which involves screening potential drugs by observing their effects on fluorescent **PPi** probes, such as **$ZnCl_2L$** complexes, to monitor **PPi** levels. Fluorescence molecules are widely used to study protein-protein titrations, and we can observe the fluorescence intensity or emission wavelength when proteins interact by using **$ZnCl_2L$** complexes as a fluorescent dye.

Supporting Information

SYNTHESIS OF WATER SOLUBLE TERPYRIDINE-LIGANDS TO STUDY AND OPTIMIZE ITS USE IN BIOIMAGING

Kiante Raqui Graham
Thesis Defense, M.S.-Chemistry
Western Carolina University (Nov. 2024)
Dr. Brian Dinkelmeyer, Dr. Jamie Wallen, Dr. Al Fischer

Characterization of Terpyridine and Zinc dichloride terpyridine complexes.

4-(4-dimethylyaminophenyl)-2,2':6',2"terpyrdine ((L_1)

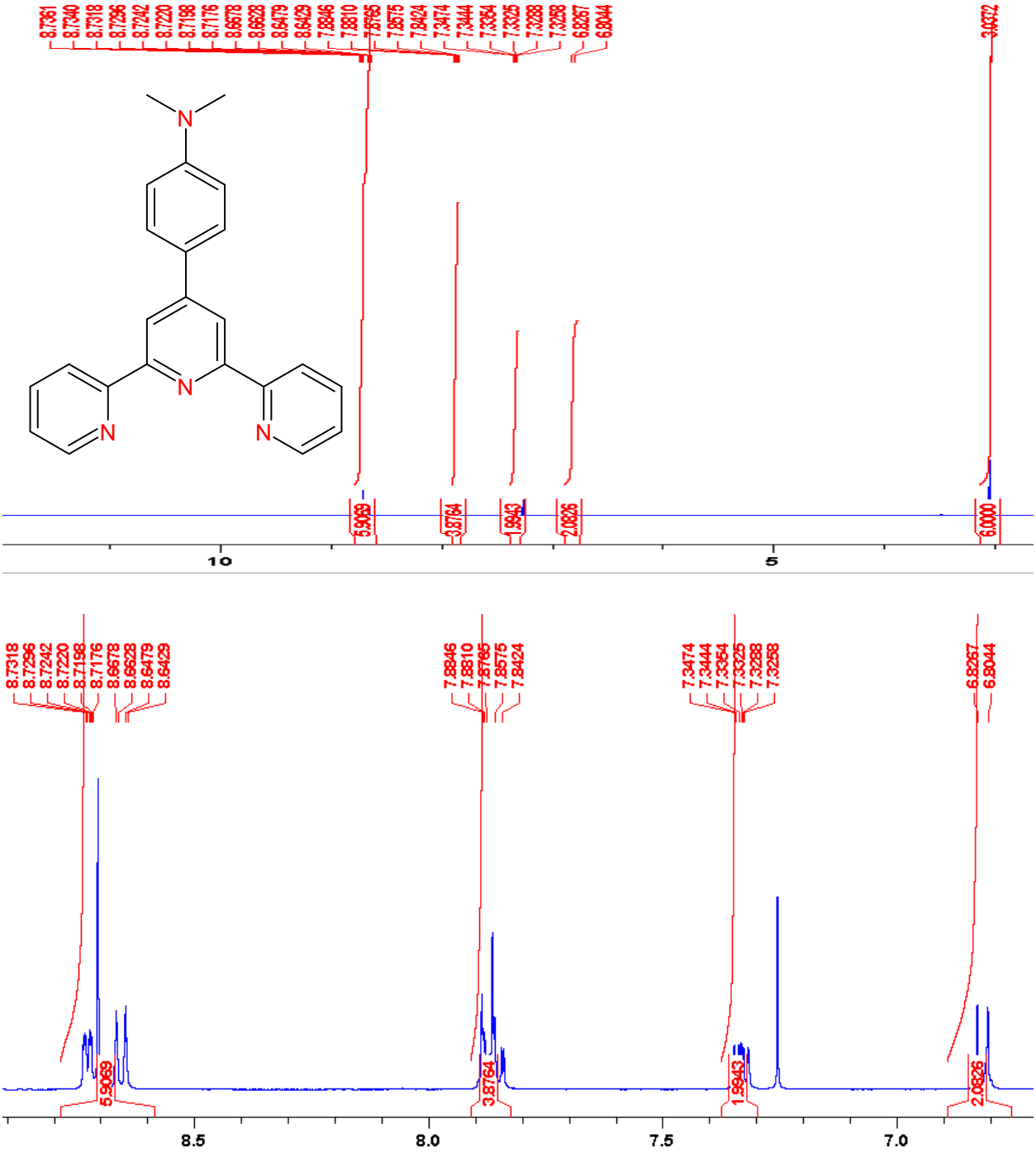

Figure 20. The ^{1}H NMR spectrum of **L_1** in $CDCl_3$.

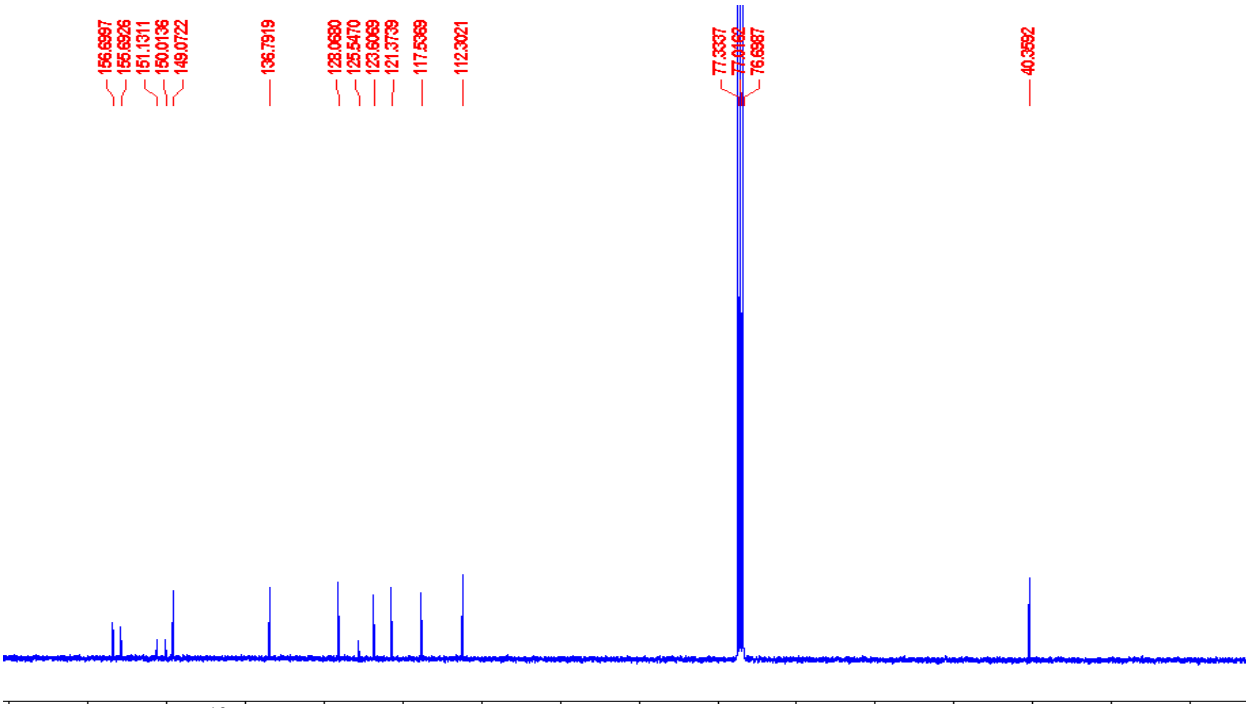

Figure 21. The ^{13}C NMR spectrum of $\mathbf{L_1}$ in $CDCl_3$.

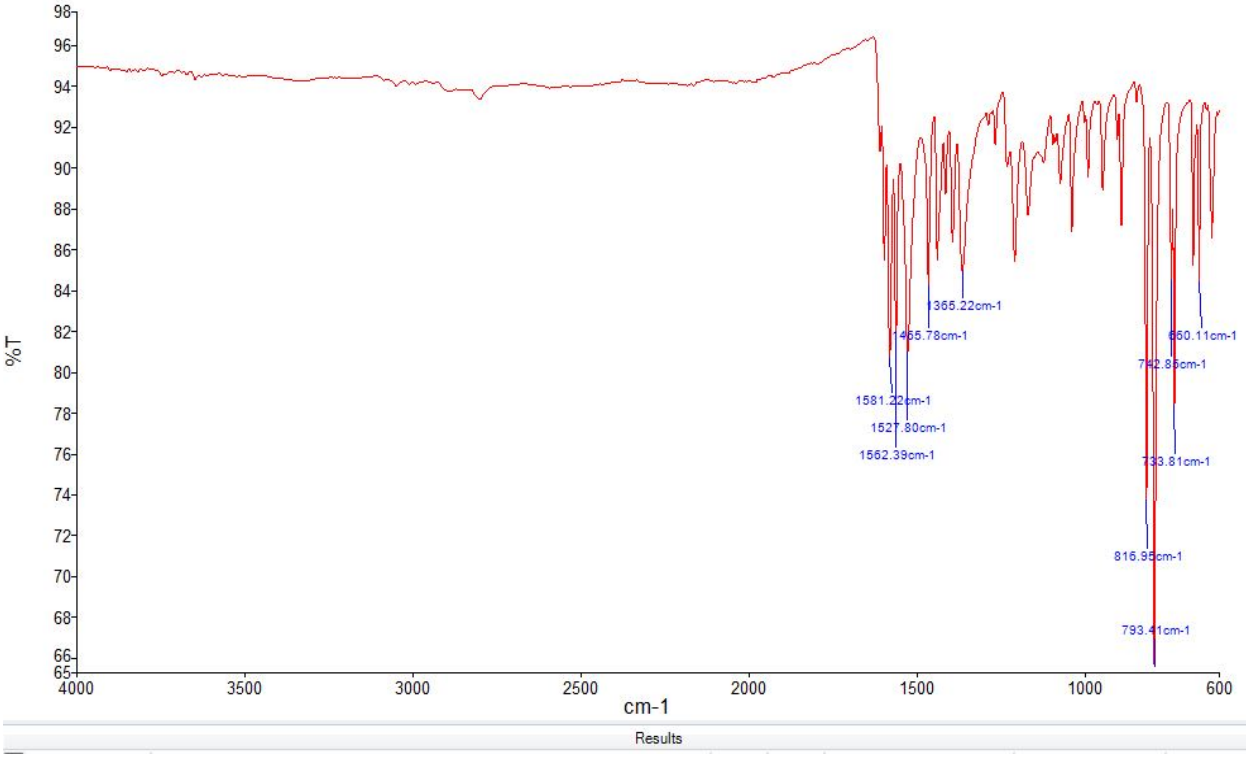

Figure 22. The FTIR spectrum of $\mathbf{L_1}$.

Zinc dichloride 4-(4-dimethylyaminophenyl)-2,2':6',2"terpyrdine ($ZnCl_2L_1$)

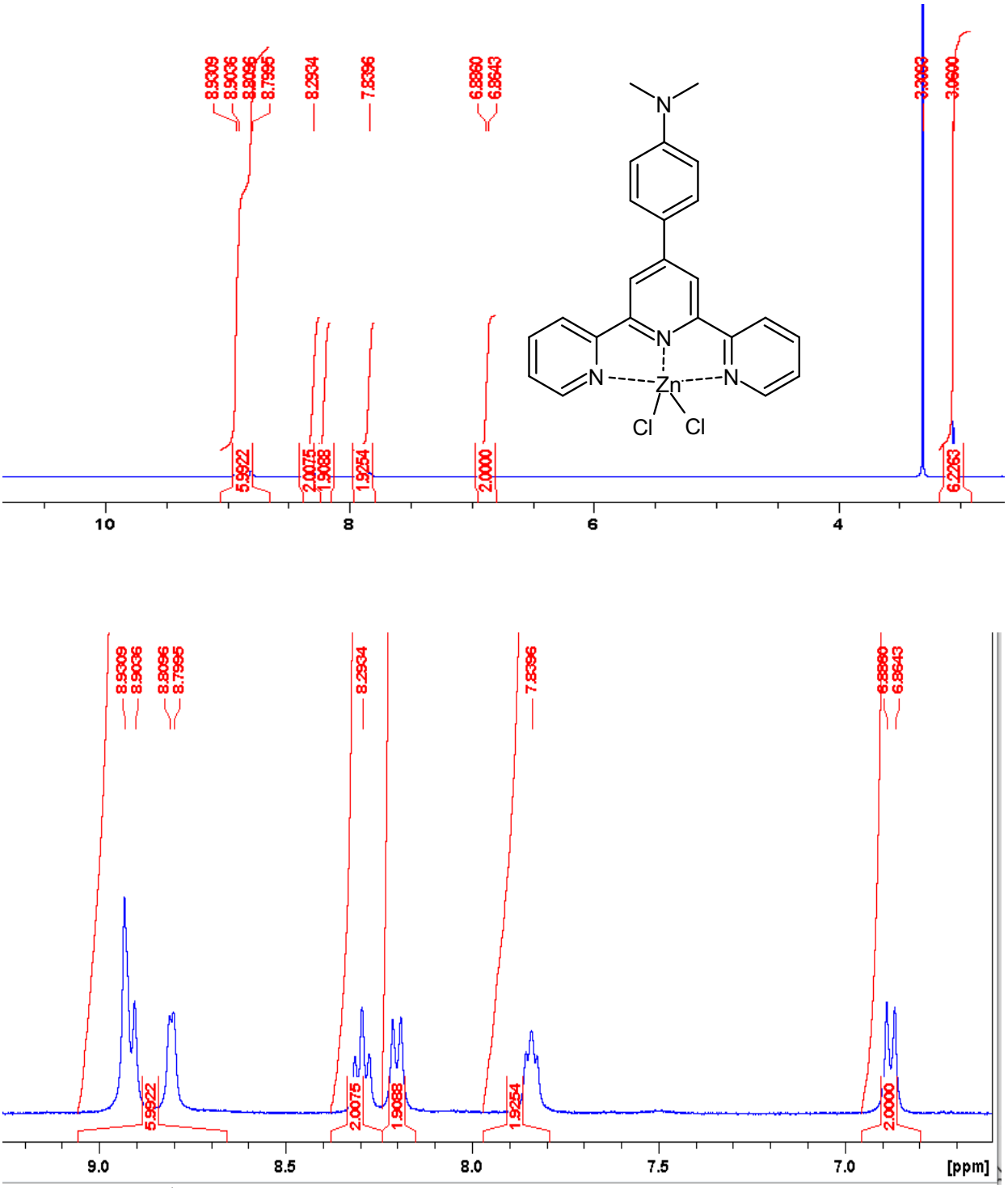

Figure 23. The ^{1}H NMR spectrum of **($ZnCl_2L_1$)** in DSMO.

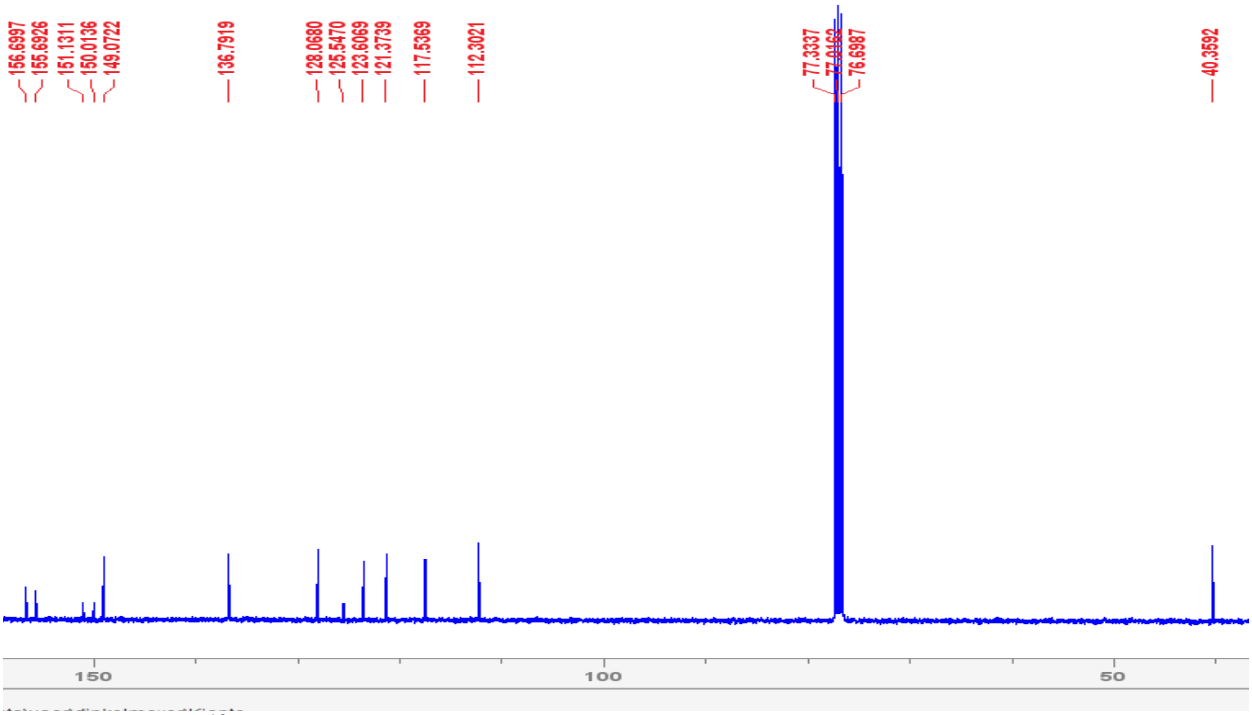

Figure 24. The ^{13}C NMR spectrum of **($ZnCl_2L_1$)** in DSMO.

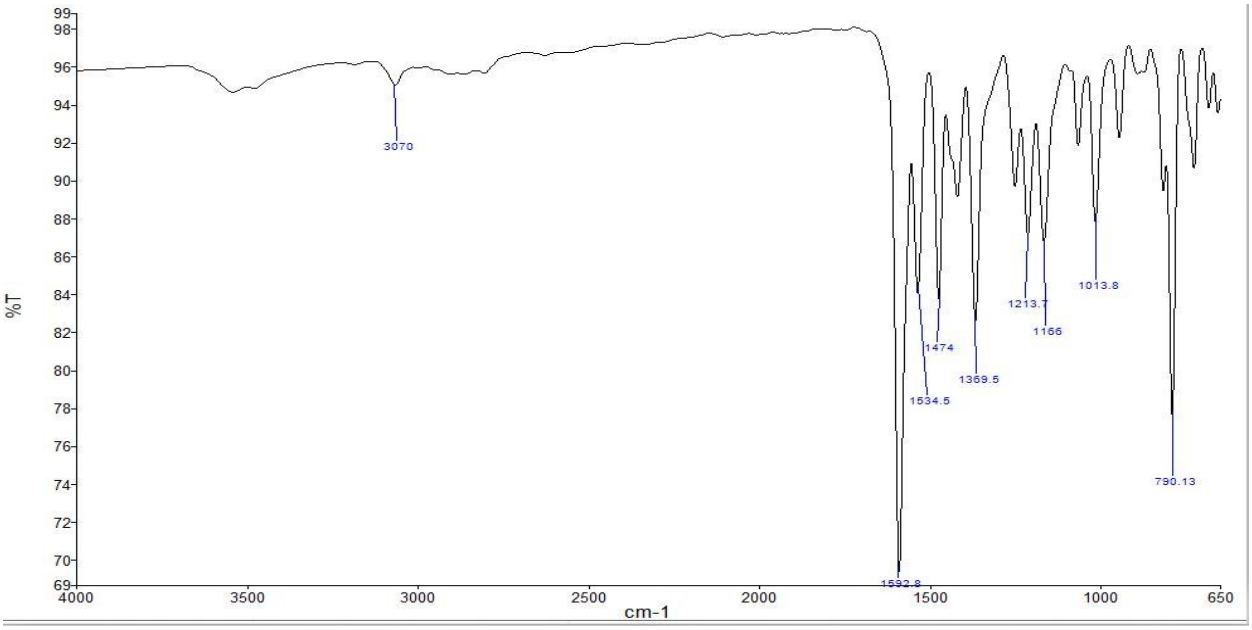

Figure 25. The FTIR spectrum of **($ZnCl_2L_1$)**.

4-(4-morpholinephenyl)-2,2’:6’,2”terpyridine (L_2)

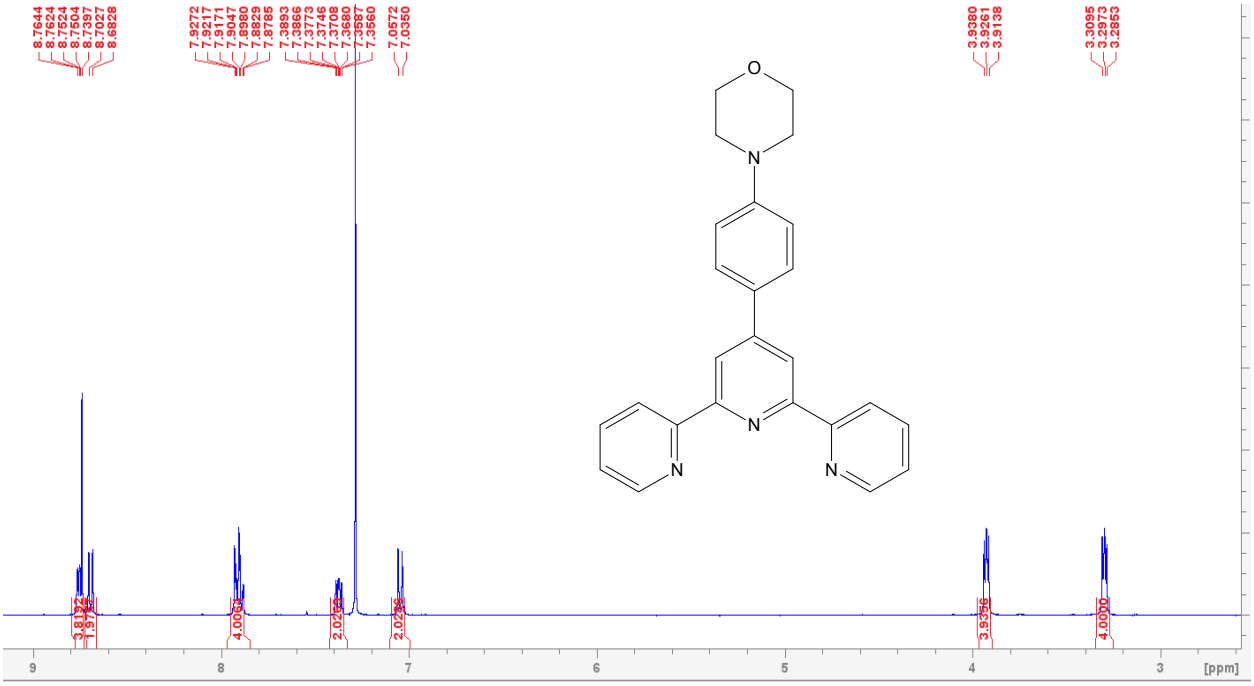

Figure 26. The ^{1}H NMR spectrum of (**L_2**)in $CDCl_3$.

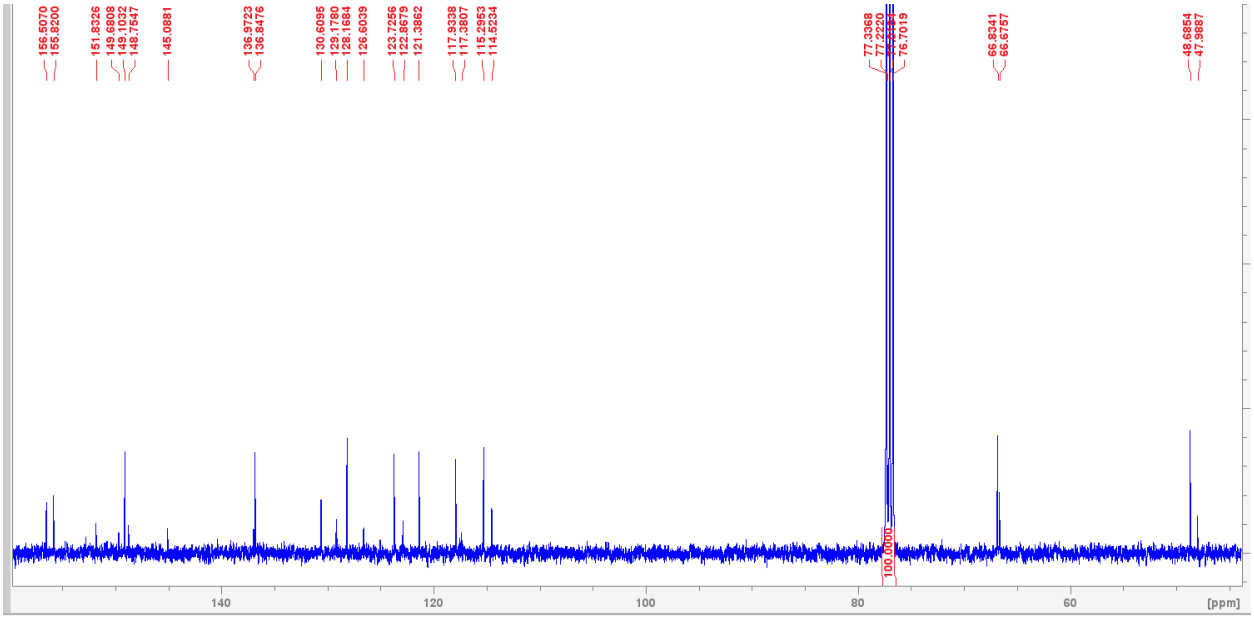

Figure 27. The ^{13}C NMR spectrum of **L_2** in DSMO.

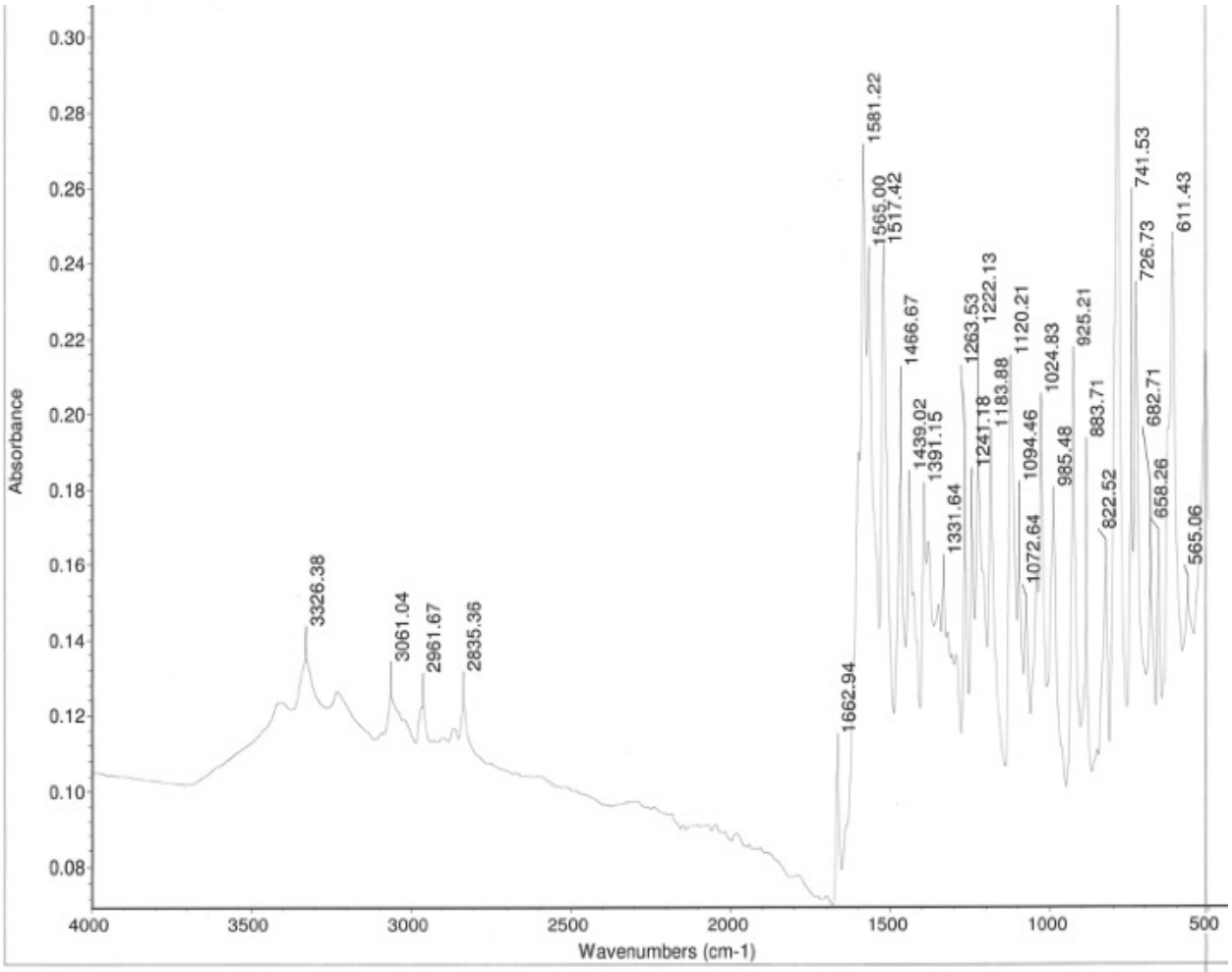

Figure 28. The FTIR spectrum of $\mathbf{L_2}$.

Zinc dichloride (4-(4-morpholinephenyl)-2,2':6',2"terpyridine) ($ZnCl_2L_2$)

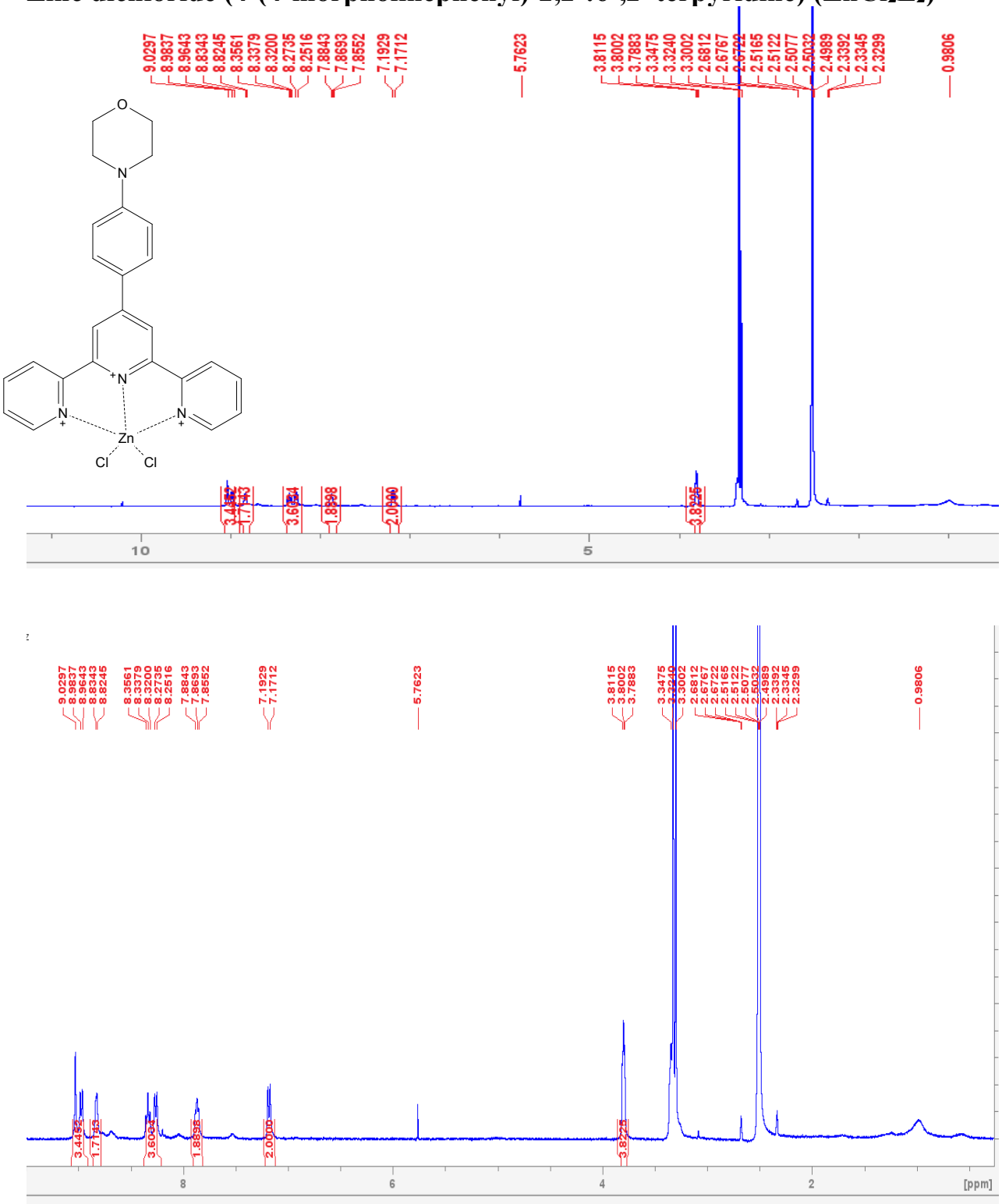

Figure 29. The ^{1}H NMR spectrum of **($ZnCl_2L_2$)** in DSMO.

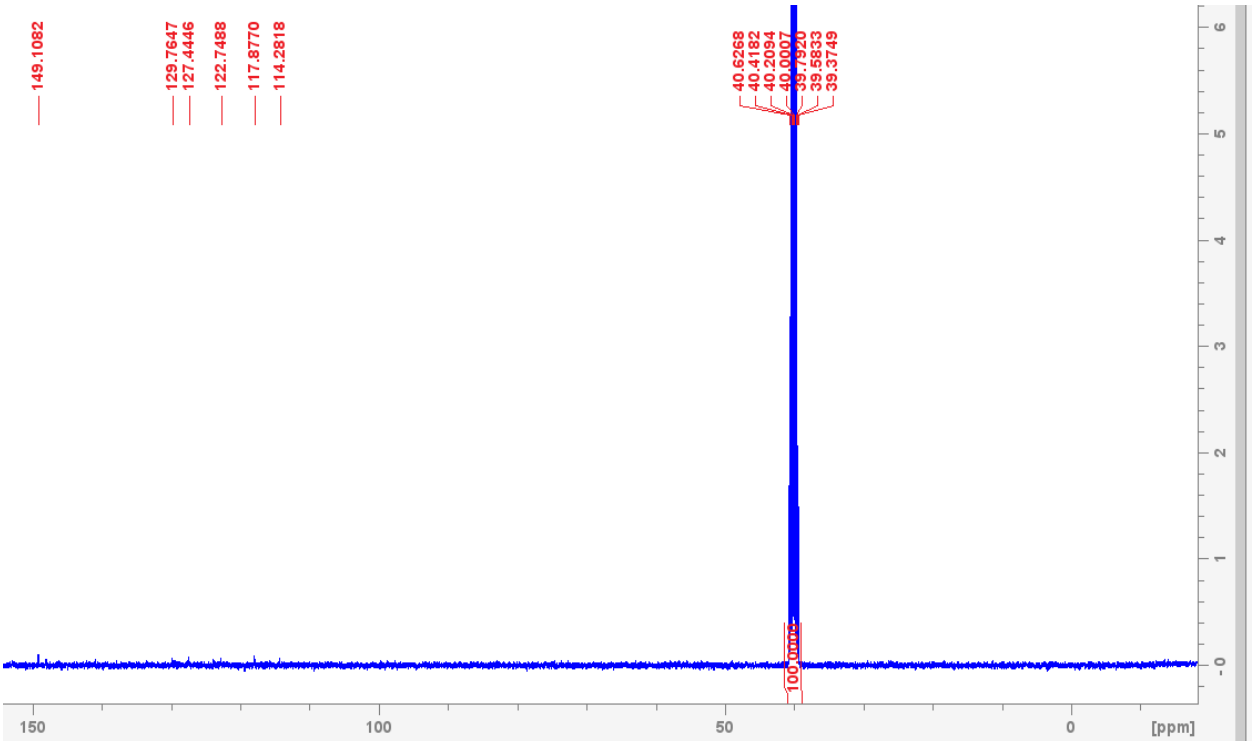

Figure 30. The ^{13}C NMR spectrum of **($ZnCl_2L_2$)** in DMSO.

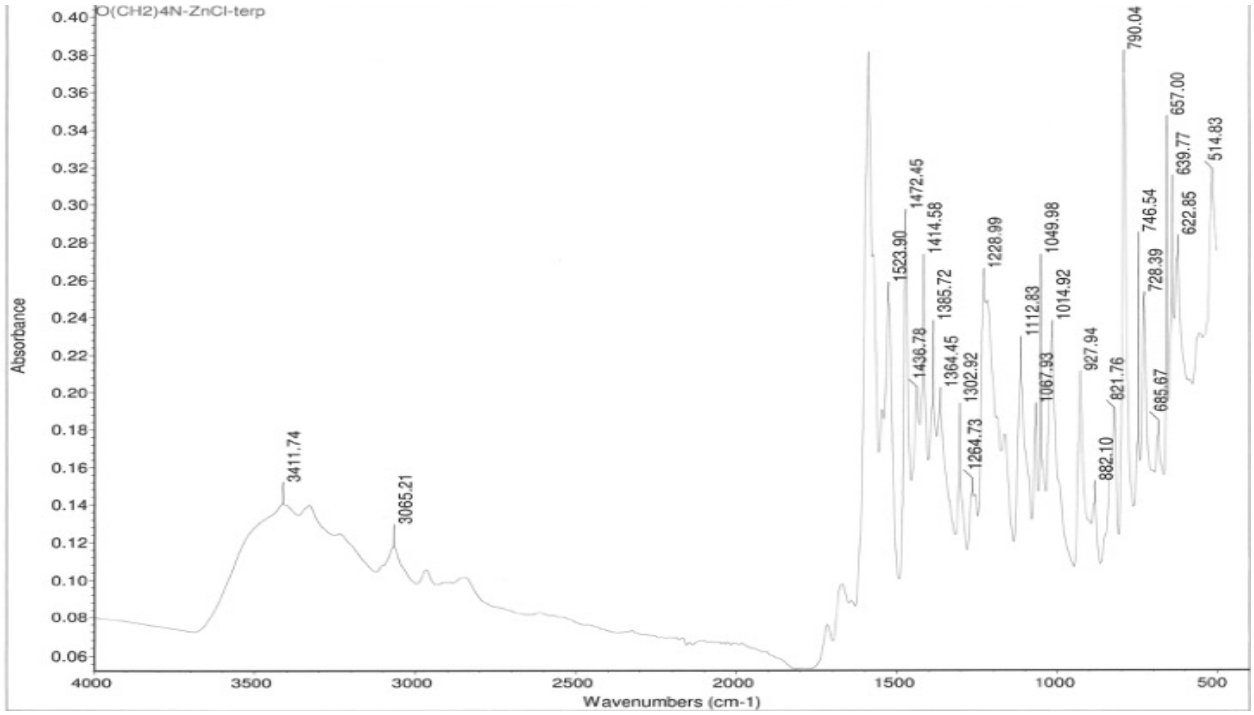

Figure 31. The FTIR spectrum of **($ZnCl_2L_1$).**

4-(4-nitrophenyl)-2,2':6',2"terpyridine (L_3)

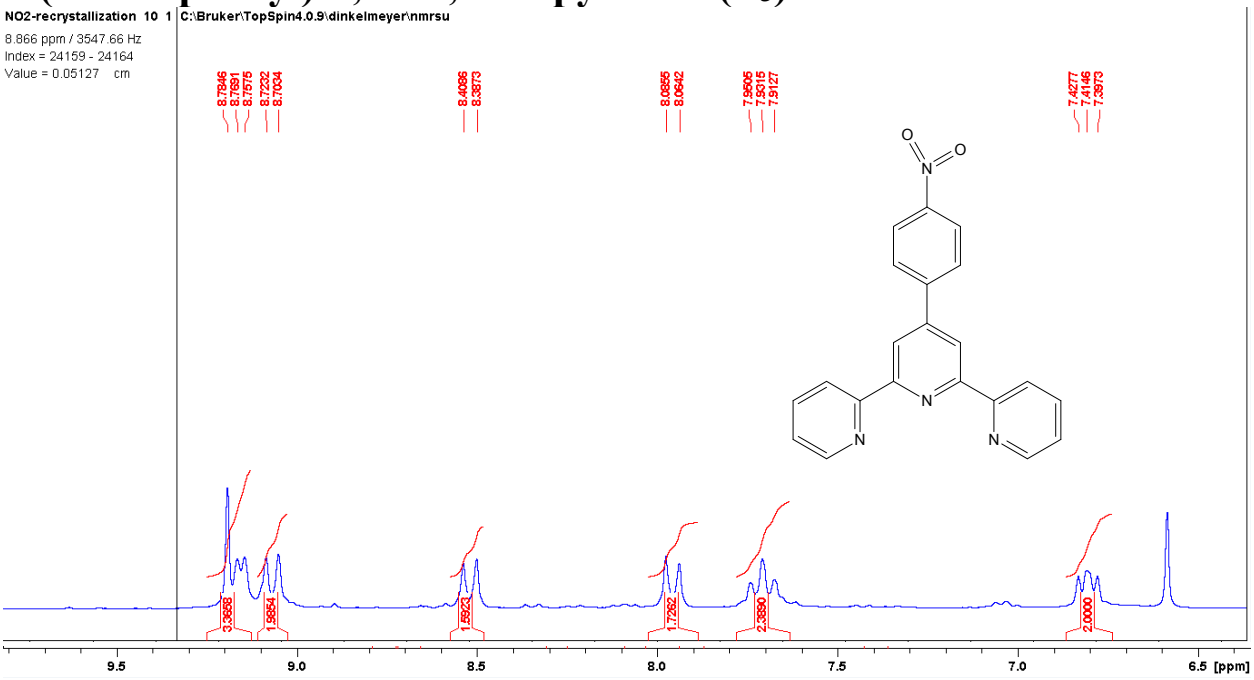

Figure 32. The ^{1}H NMR spectrum of $\mathbf{L_3}$ in $CDCl_3$.

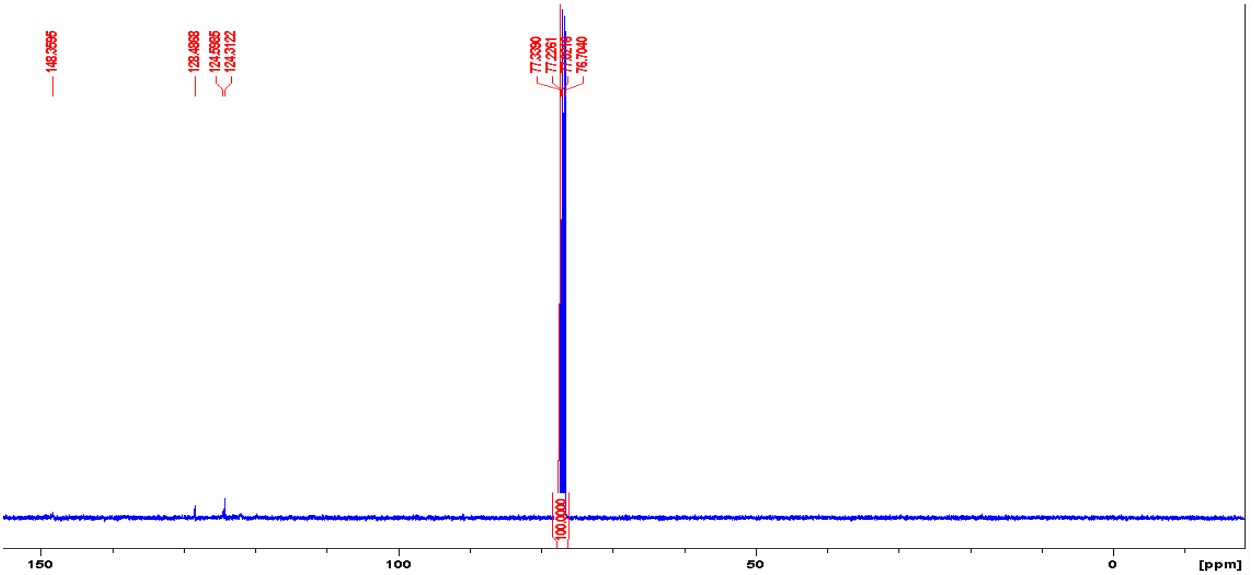

Figure 33. The ^{13}C NMR spectrum of $\mathbf{L_3}$ in DSMO.

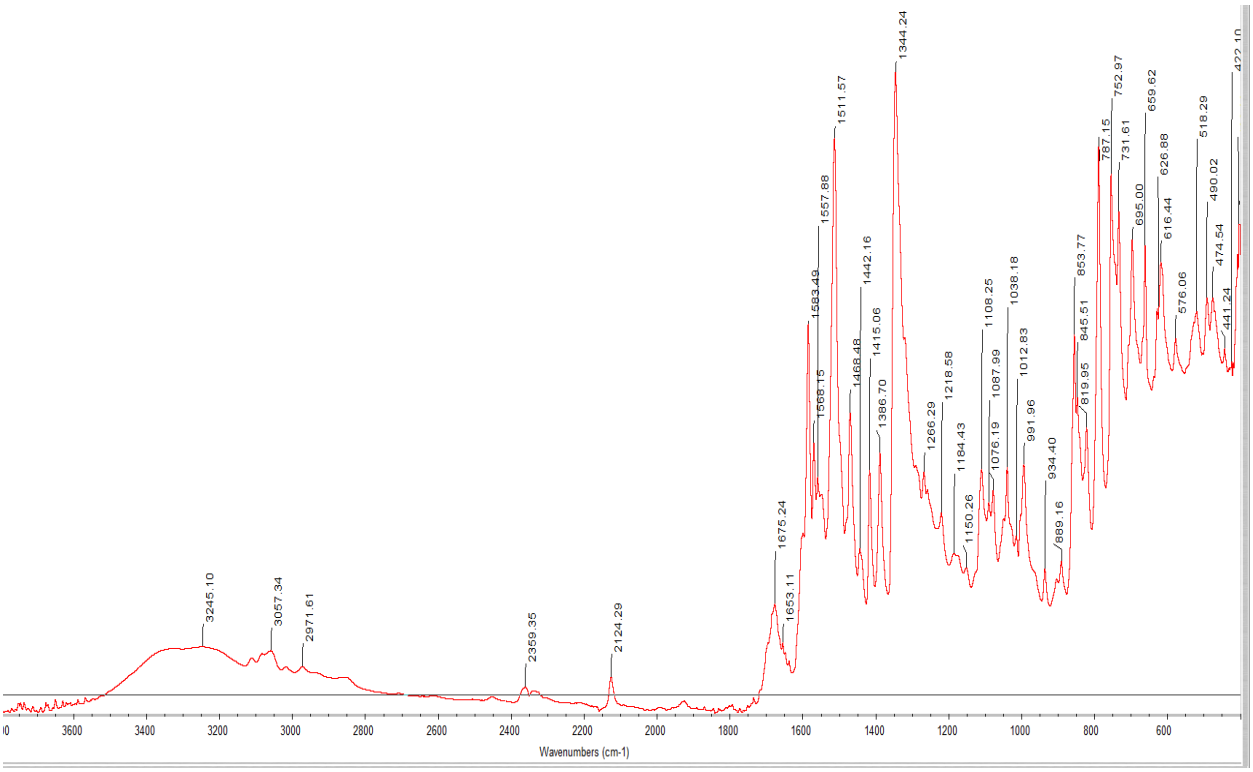

Figure 34. The FTIR spectrum of $\mathbf{L_3}$.

Zinc dichloride (4-(4-nitrophenyl)-2,2':6',2"terpyridine) ($ZnCl_2L_3$)

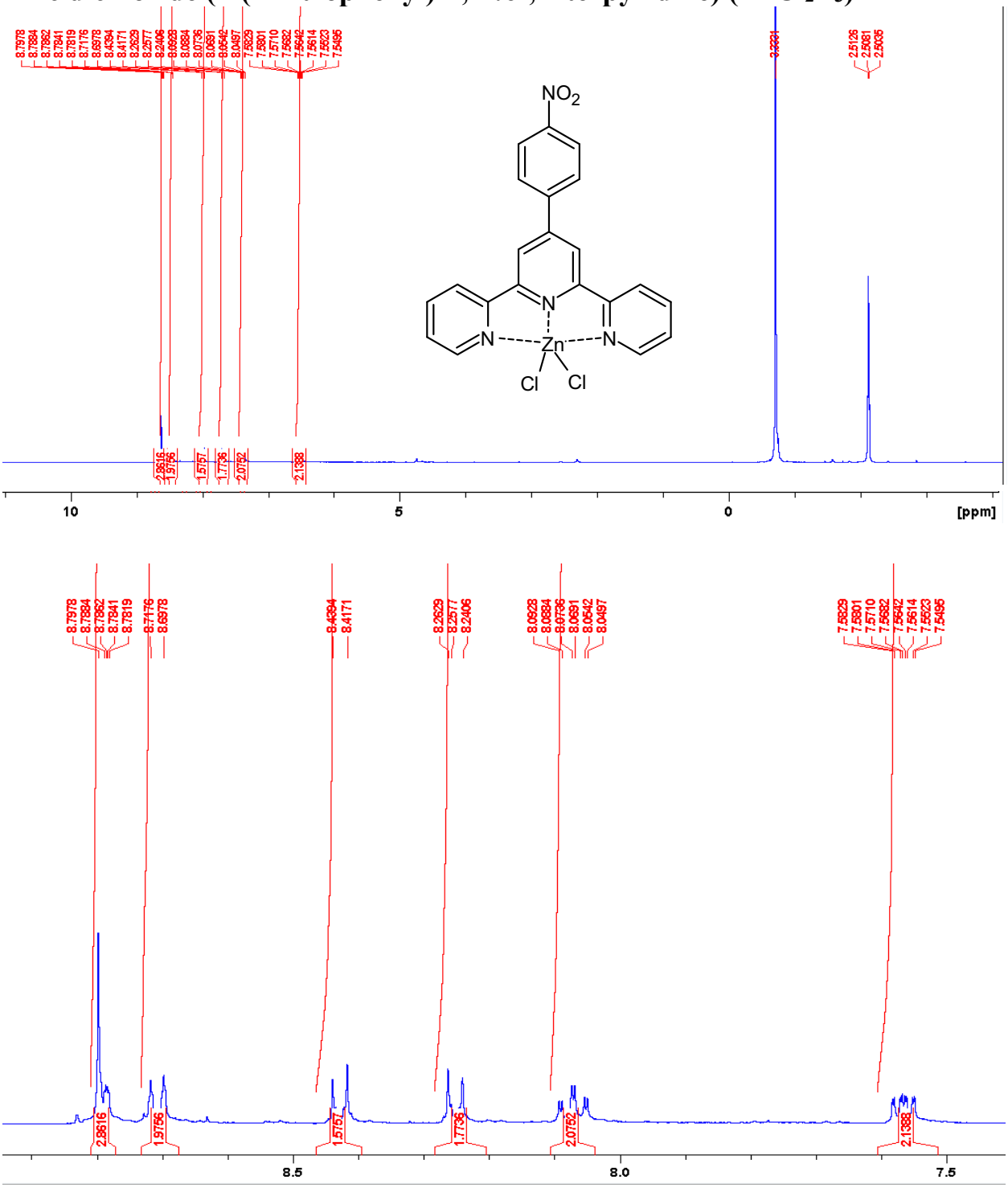

Figure 35. The ^{1}H NMR spectrum of **($ZnCl_2L_3$)** in DSMO.

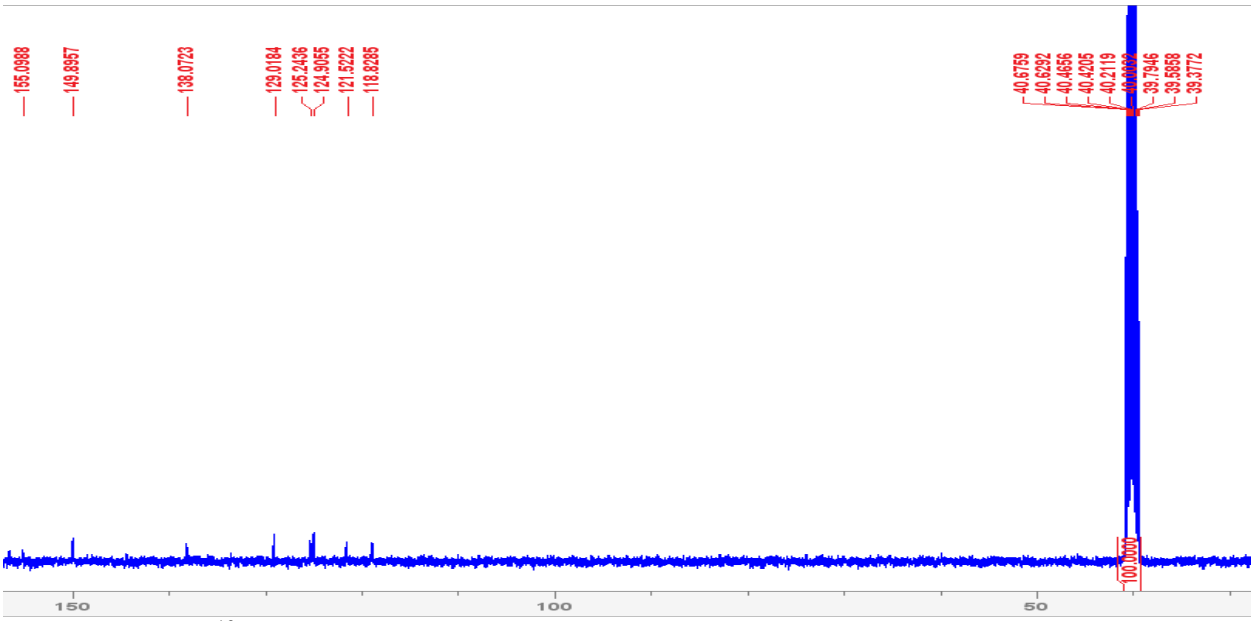

Figure 36. The ^{13}C NMR spectrum of **($ZnCl_2L_3$)** in DSMO.

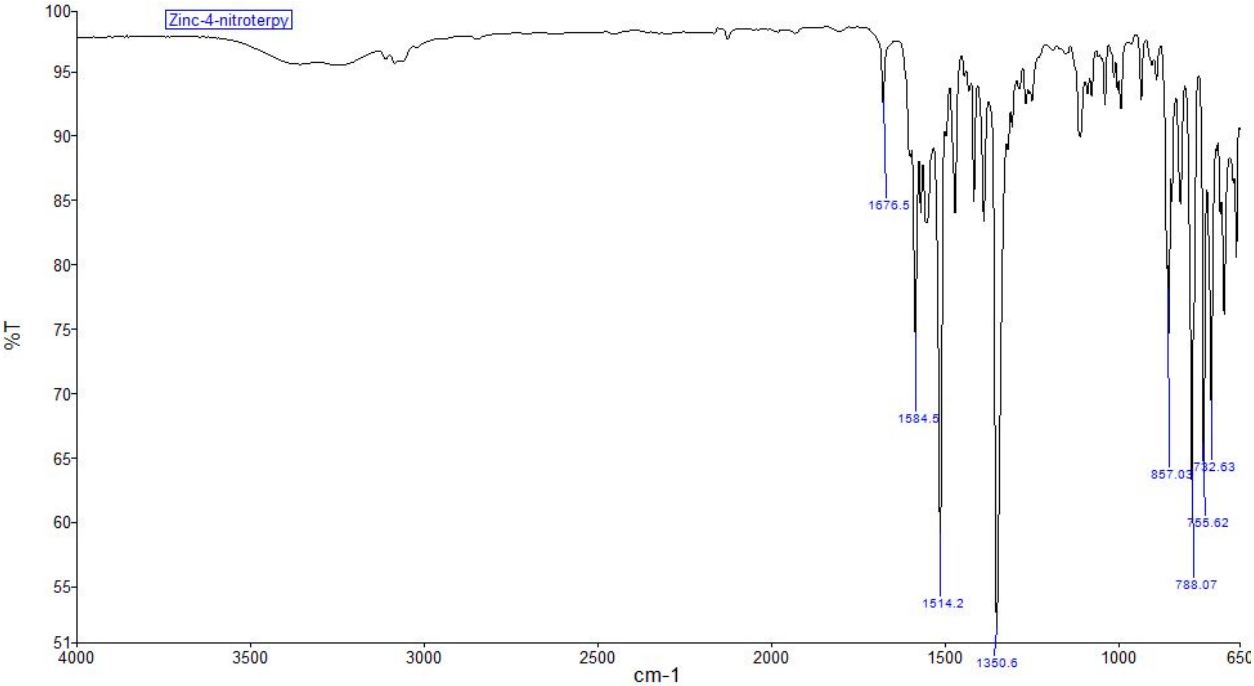

Figure 37. The FTIR spectrum of **($ZnCl_2L_3$)**.

4-(4-aminophenyl)-2,2’:6’,2”terpyridine (L_4)

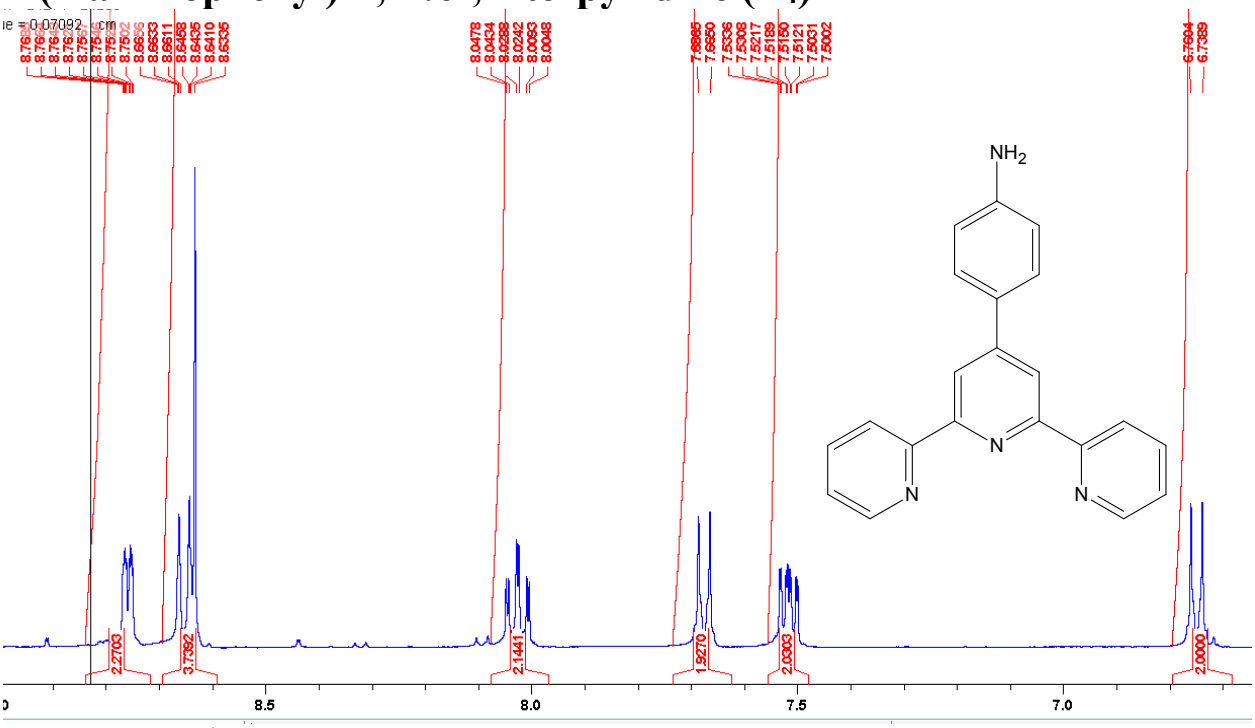

Figure 38. The ^{1}H NMR spectrum of **L_4** in $CDCl_3$.

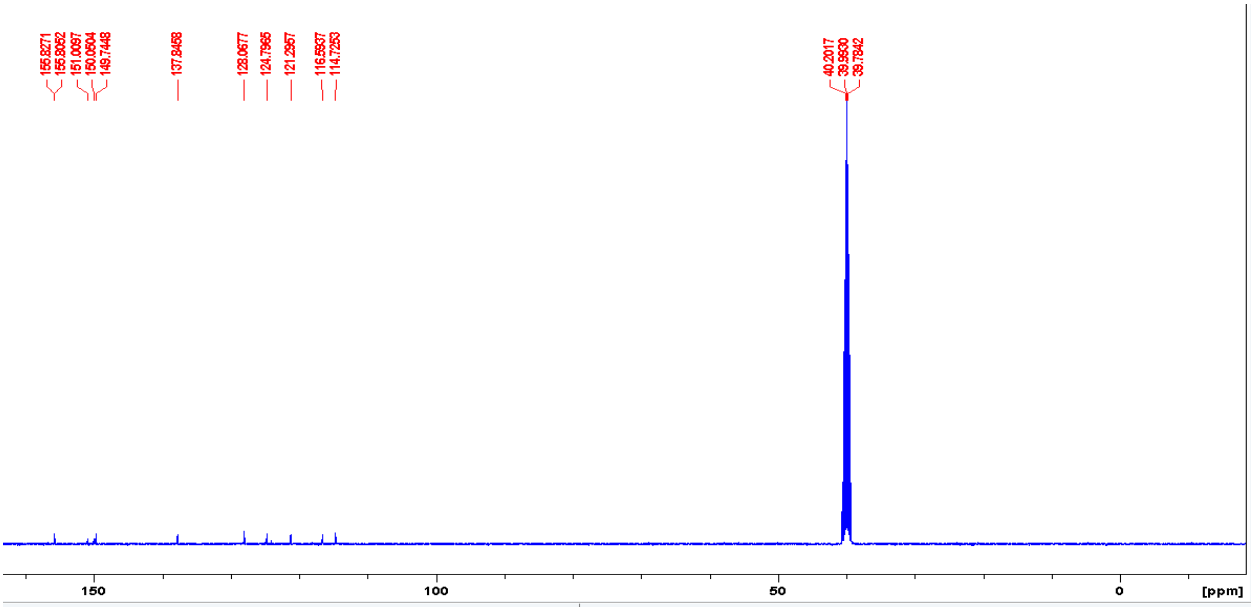

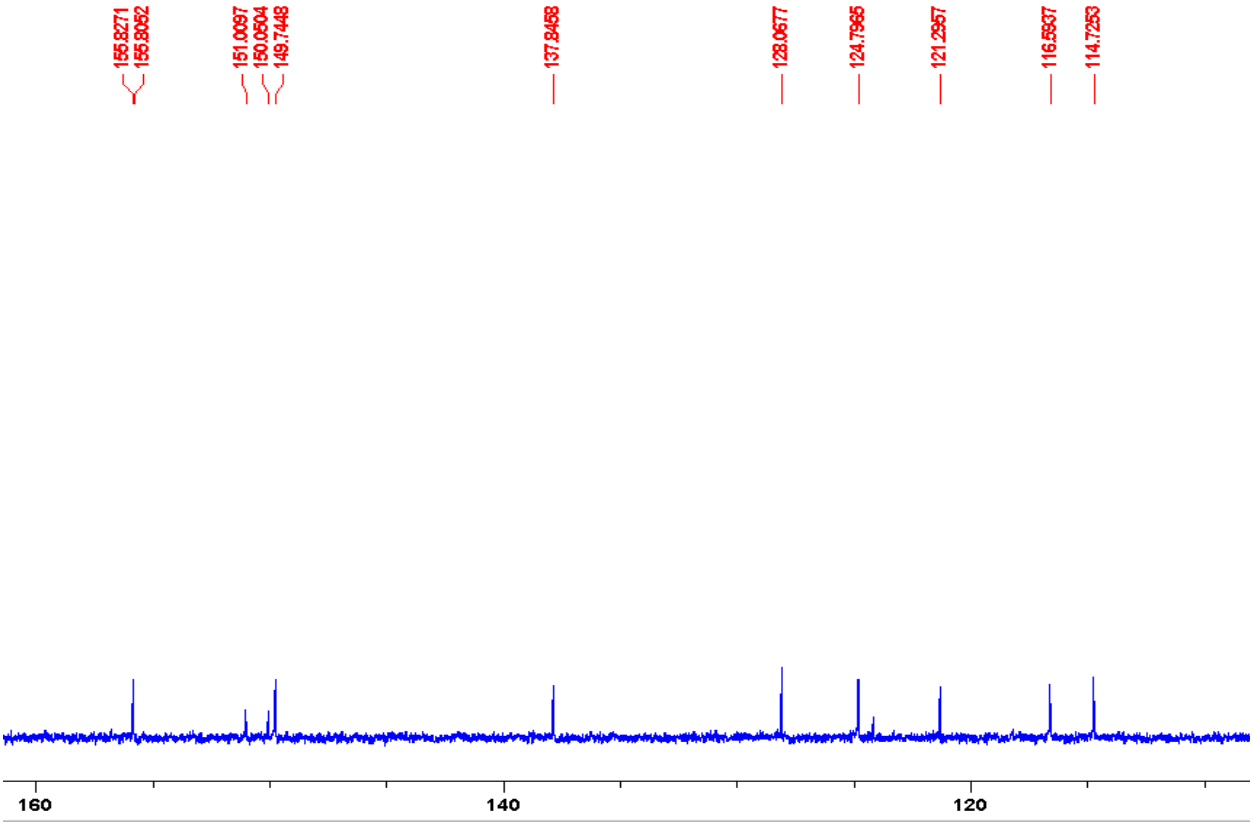

Figure 39. The ^{13}C NMR spectrum of $\mathbf{L_4}$ in DSMO.

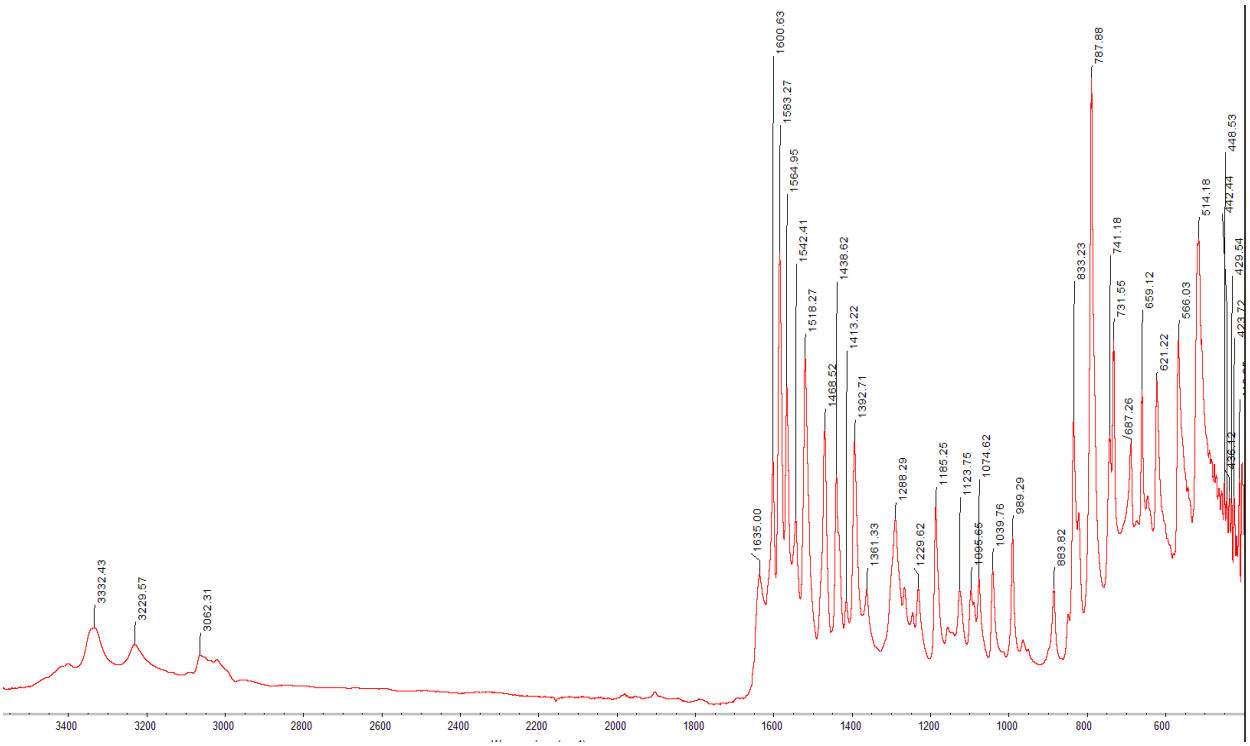

Figure 40. The FTIR spectrum of $\mathbf{L_4}$.

Zinc dichloride (4-(4-aminophenyl)-2,2':6',2"terpyridine) ($ZnCl_2L_4$)

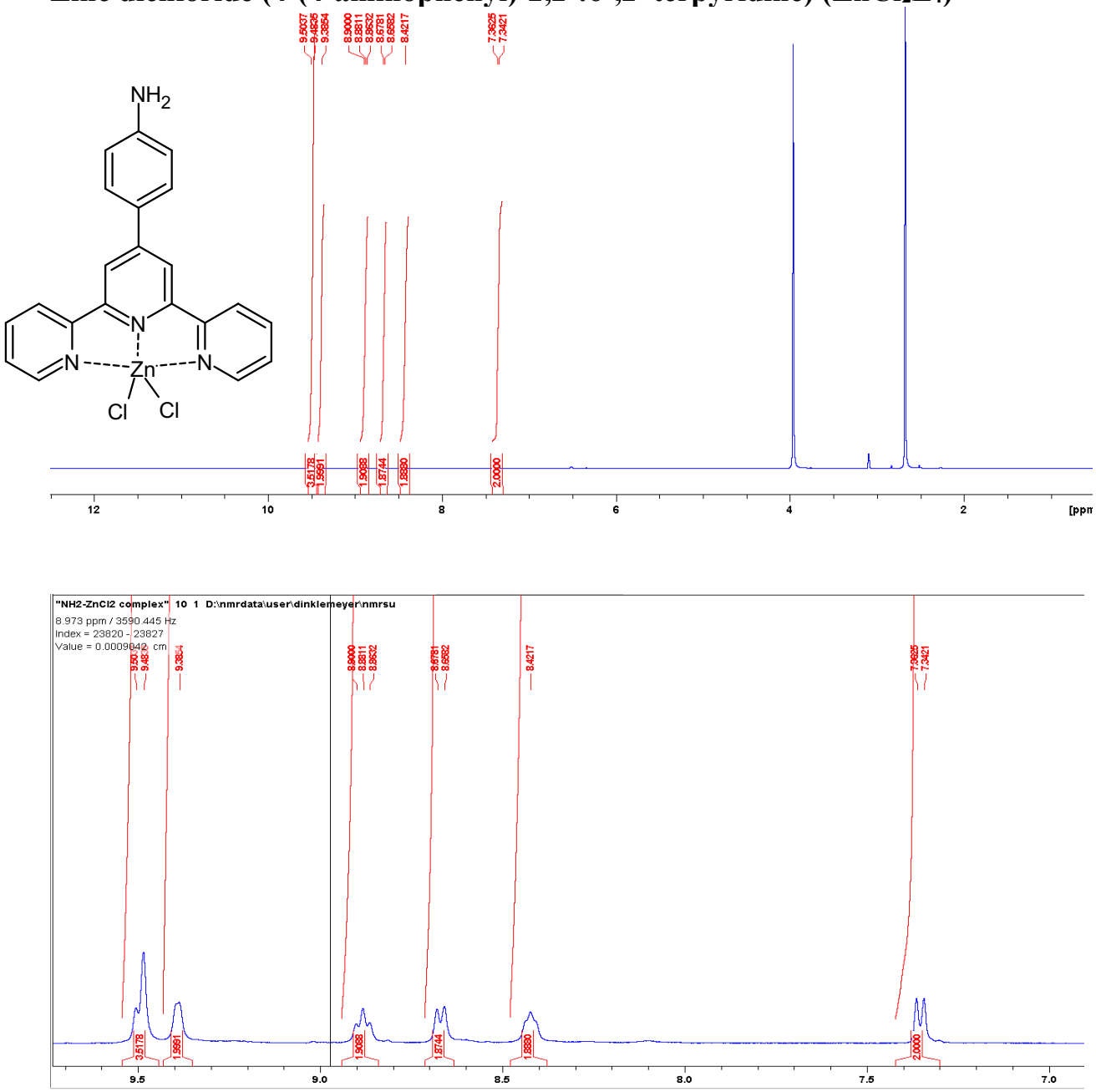

Figure 41. The ^{1}H NMR spectrum of **($ZnCl_2L_4$)** in DSMO.

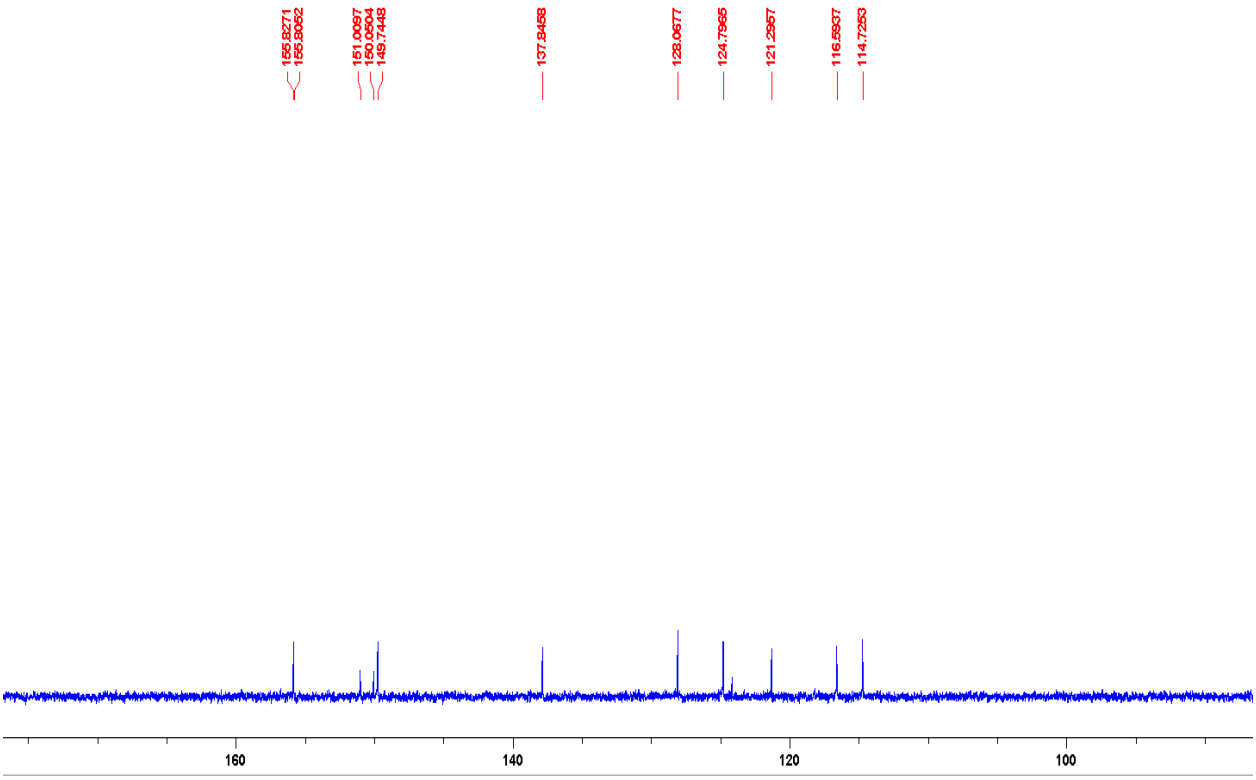

Figure 42. The ^{13}C NMR spectrum of **($ZnCl_2L_4$)** in DSMO.

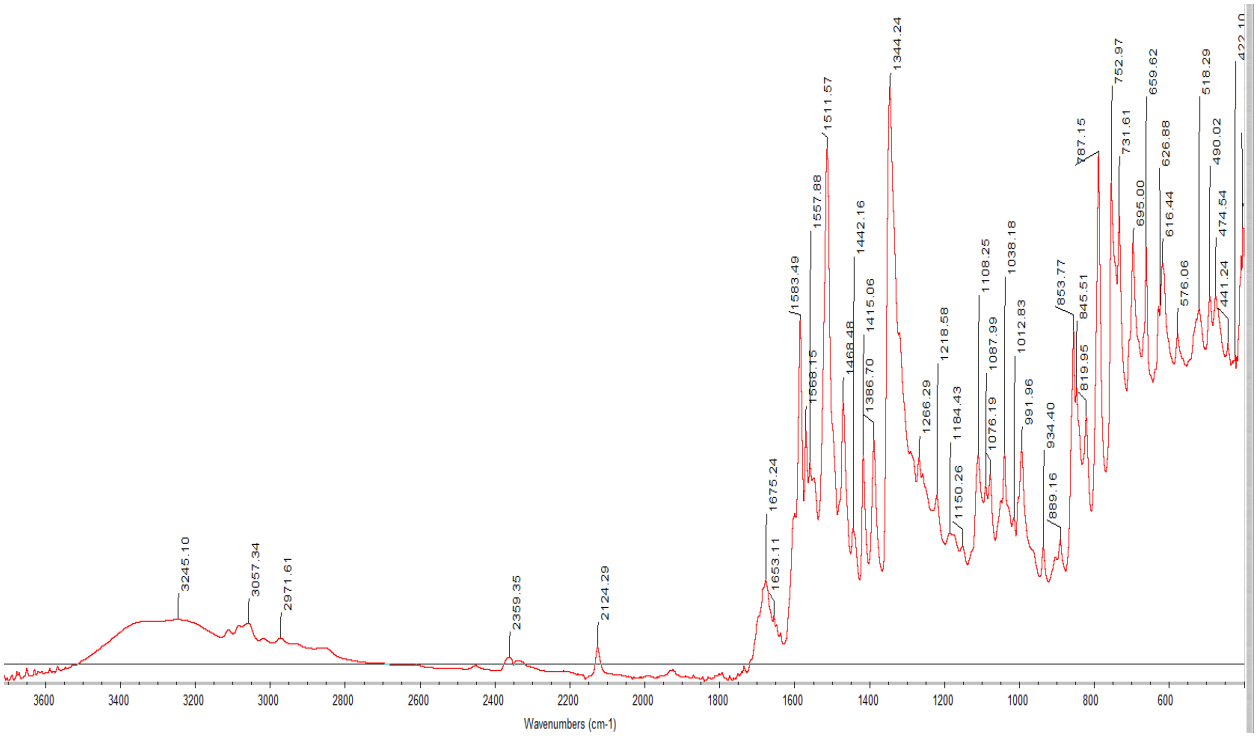

Figure 43. The FTIR spectrum of **($ZnCl_2L_4$).**

4-(4-hydroxyl)-2,2':6',2"terpyridine (L_5)

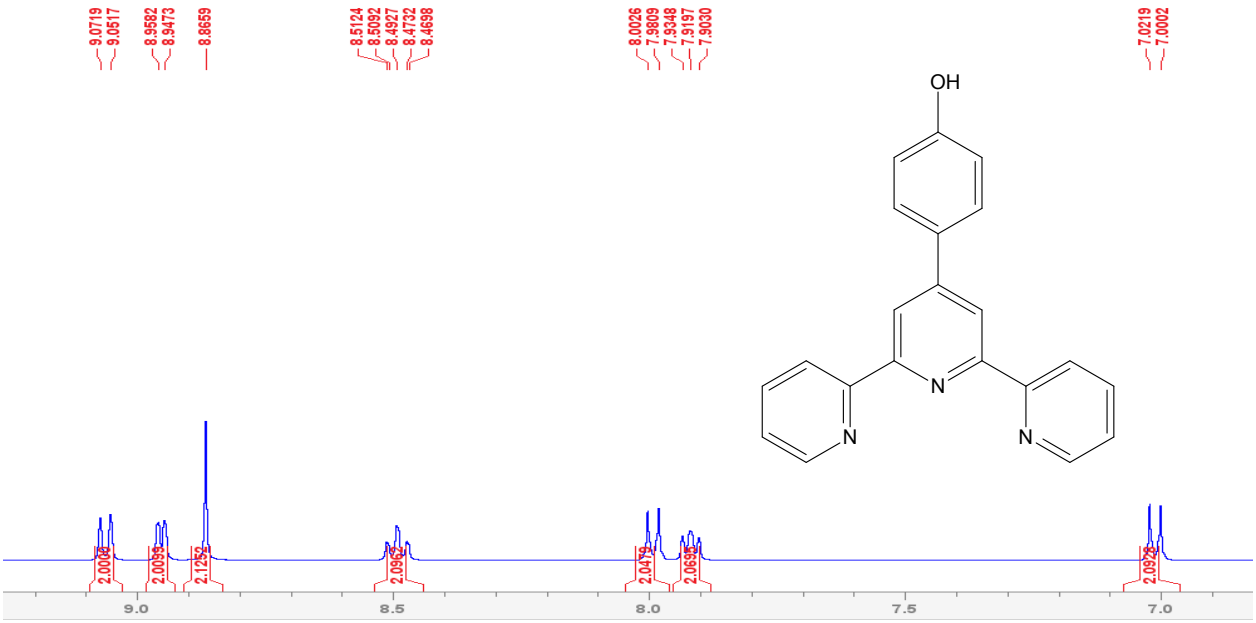

Figure 44. The ^{1}H NMR spectrum of L_5 in DSMO.

*$ZnCl_2L_{1-4}$ COMPLEXES **PPi** TITRATION STUDIES*

Well No.	1	2	3	4	5	6	7	8	9	10	11	12
PPi (uL)	0	30	60	75	90	120	150	180	210	240	270	300
$ZnCl_2L$ (uL)	300	270	240	225	210	180	150	120	90	60	30	0
Mole fraction **PPi**	0	0.1	0.2	0.25	0.3	0.40	0.5	0.6	0.7	0.8	0.9	1.00

Table 1. 96 well plate(max volume is 300uL) is prepared with 100uM **$ZnCl_2L$** and 100 uM **PPi** solution with varying volumes in replicates of three. Row 4 is the 3:1 ratio of **$ZnCl_2L$** and **PPi** anion.

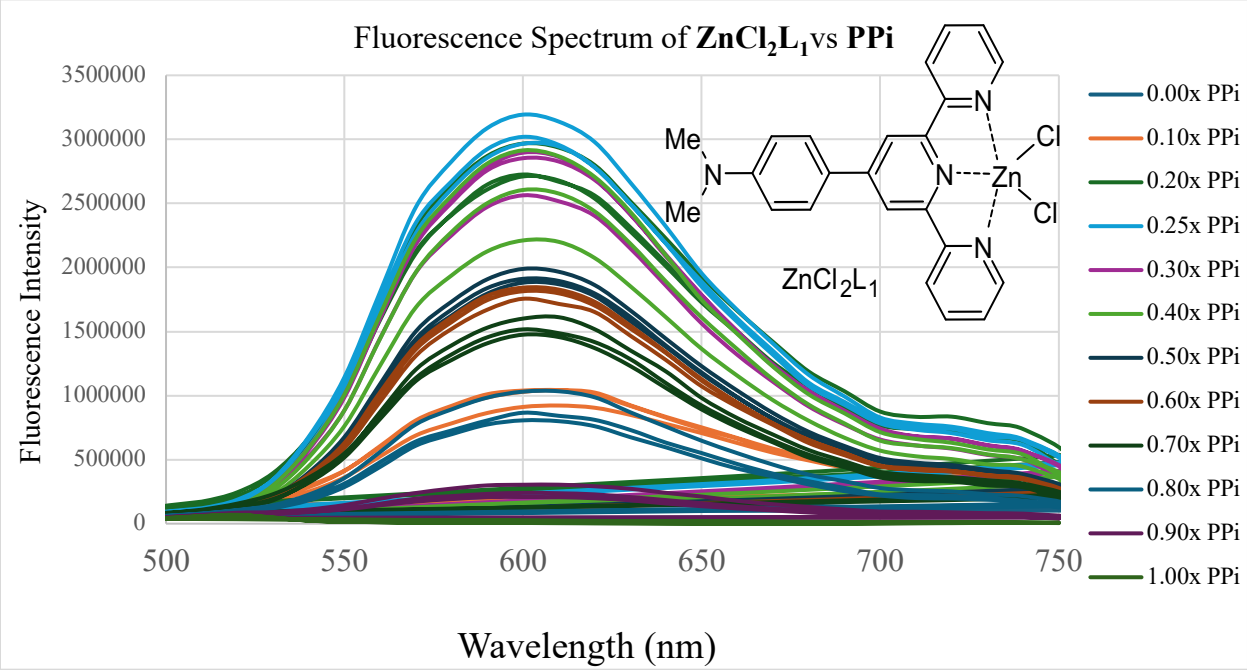

Figure 11a. Fluorescence spectrum of **$ZnCl_2L_1$** (100uM) [excitation 440nm and emissions 591nm] at varying volumes upon addition of **PPi**(100uM) at varying volumes in replicates of three.

Graph 11b. A Job Plot analysis for **PPi** binding to **$ZnCl_2L_1$** (100uM) [excitation 440nm and emissions 591nm] at a 1:3 ratio in HEPES buffer (pH 7.4).

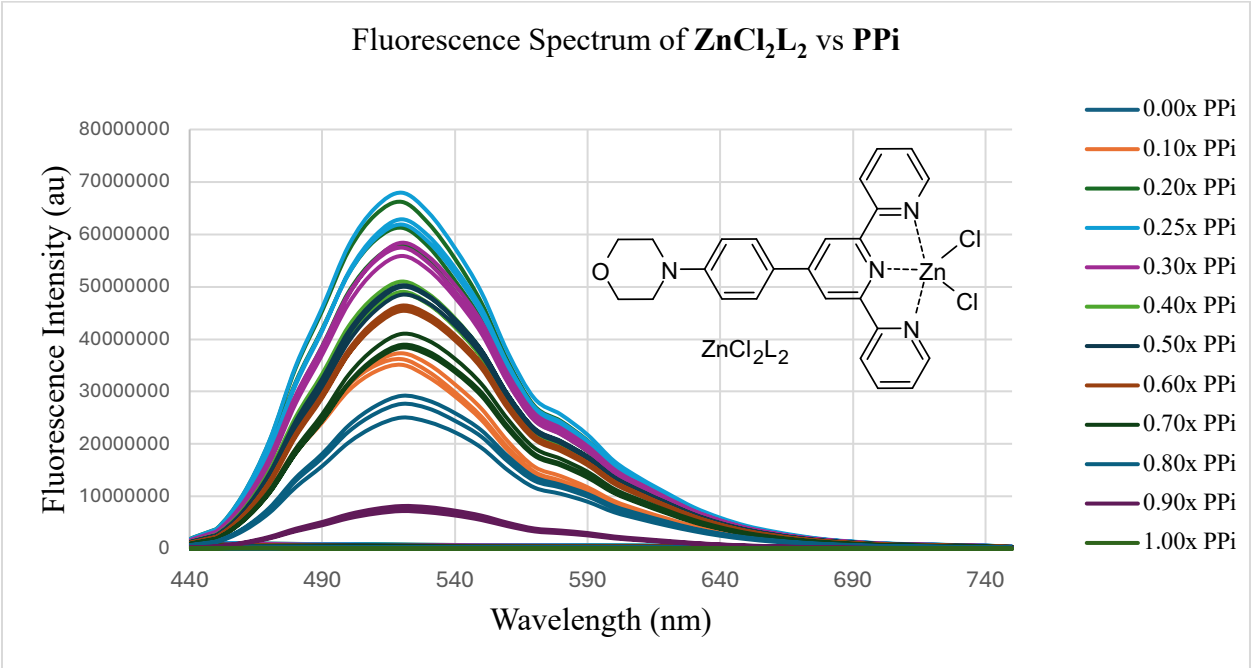

Figure 12a. Fluorescence spectrum of **$ZnCl_2L_2$** (100uM) [excitation 400nm and emissions 520nm] at varying volumes upon addition of **PPi**(100uM) at varying volumes in replicates of three.

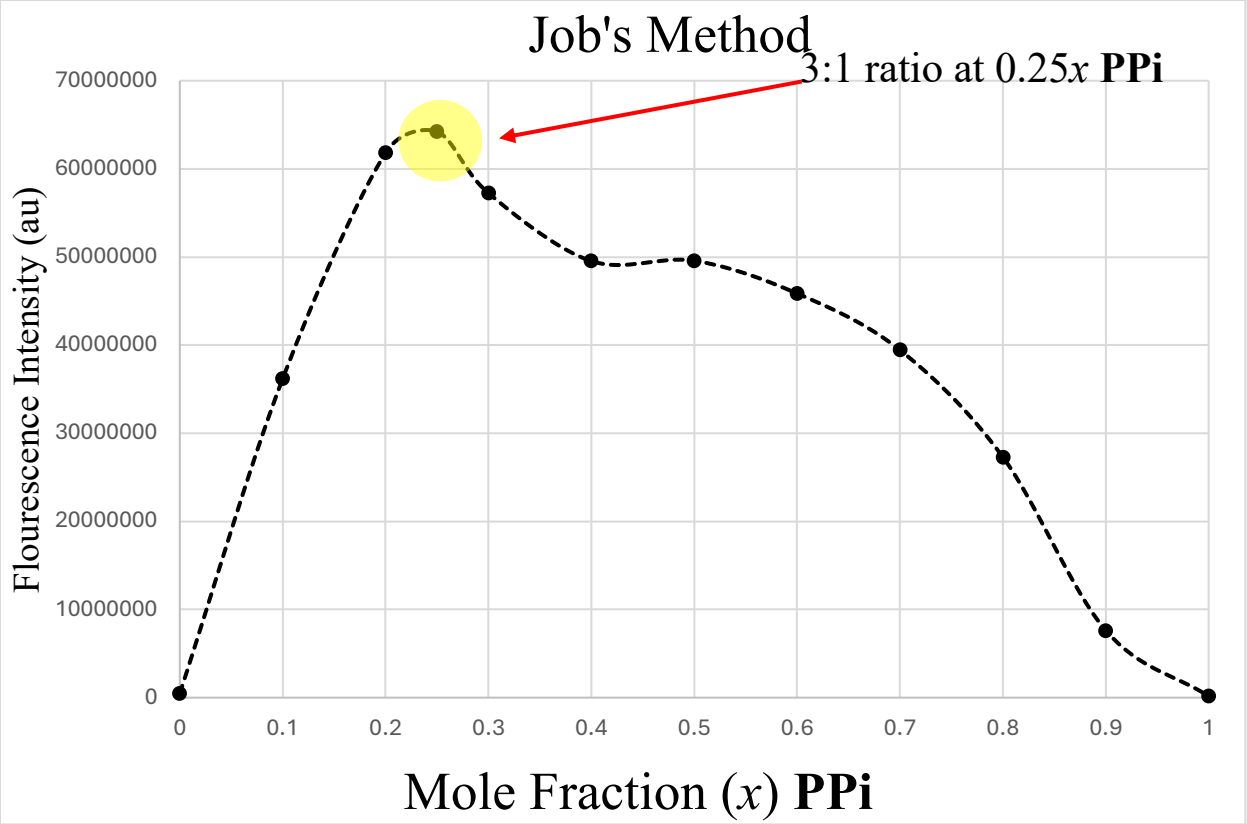

Graph 12b. A Job Plot analysis for PPi binding to **$ZnCl_2L_2$** (100uM) [excitation 400nm and emissions 520nm] at a 1:3 ratio in HEPES buffer (pH 7.4). Omitted cell 3 because it being an outlie

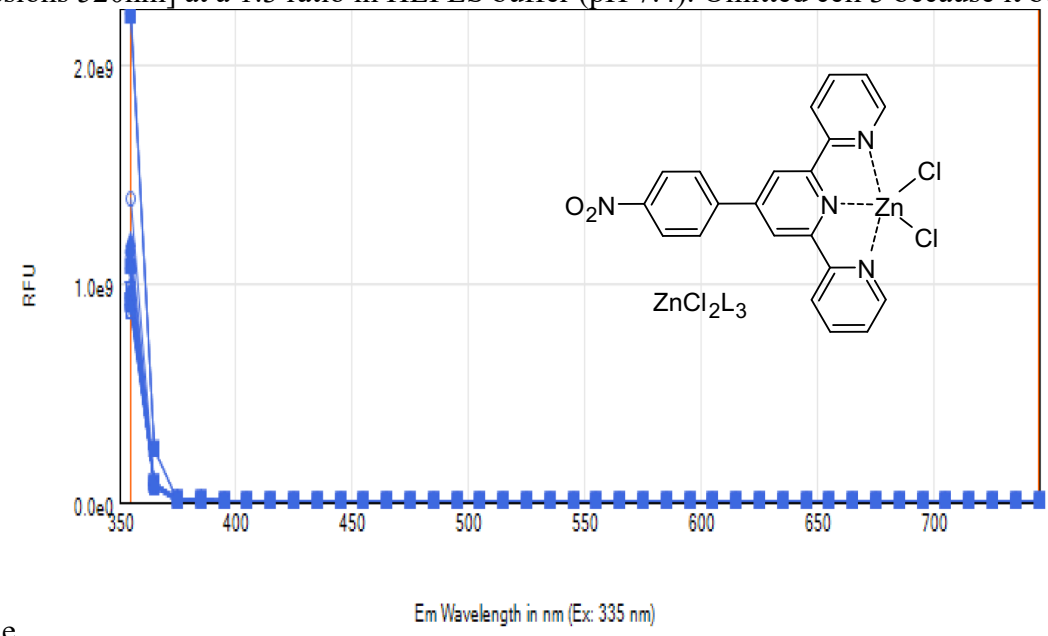

Figure 13a. Fluorescence spectra of **$ZnCl_2L_3$** (100uM) [excitation 335nm and emissions 355nm] upon addition of **PPi** (100uM) in replicates of three.

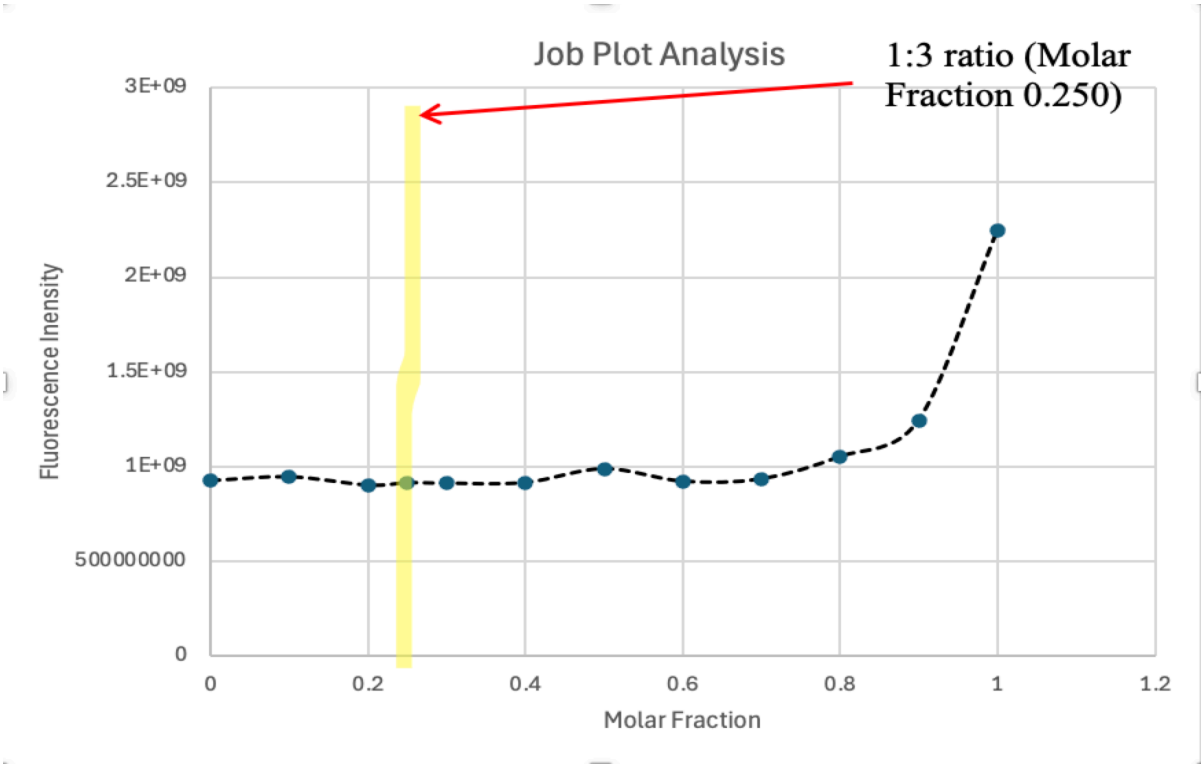

Figure 13b. A Job Plot analysis for **PPi** binding to **$ZnCl_2L_3$** (100uM)**.**[excitation 335nm and emissions 355nm] at a 1:3 ratio in HEPES buffer (pH 7.4).

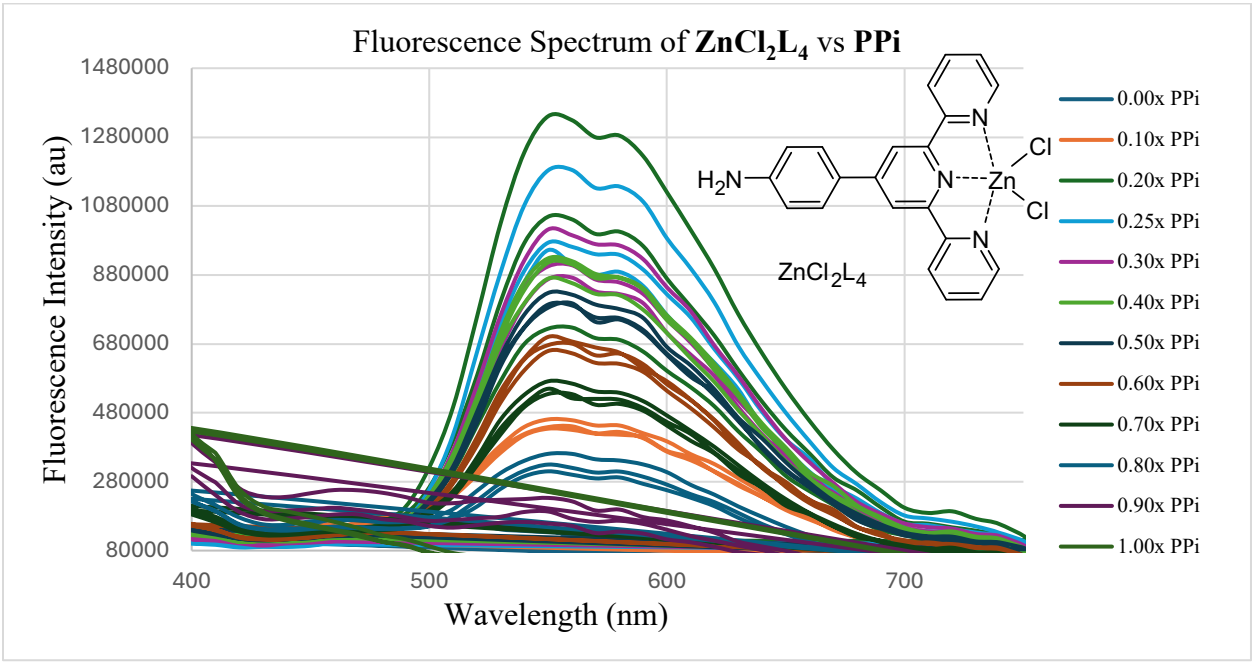

Figure 14a. [excitation 350nm and emissions 570nm] **a)**Fluorescence spectrum of **$ZnCl_2L_4$** (100uM) upon addition of **PPi** (100uM) in replicates of three.

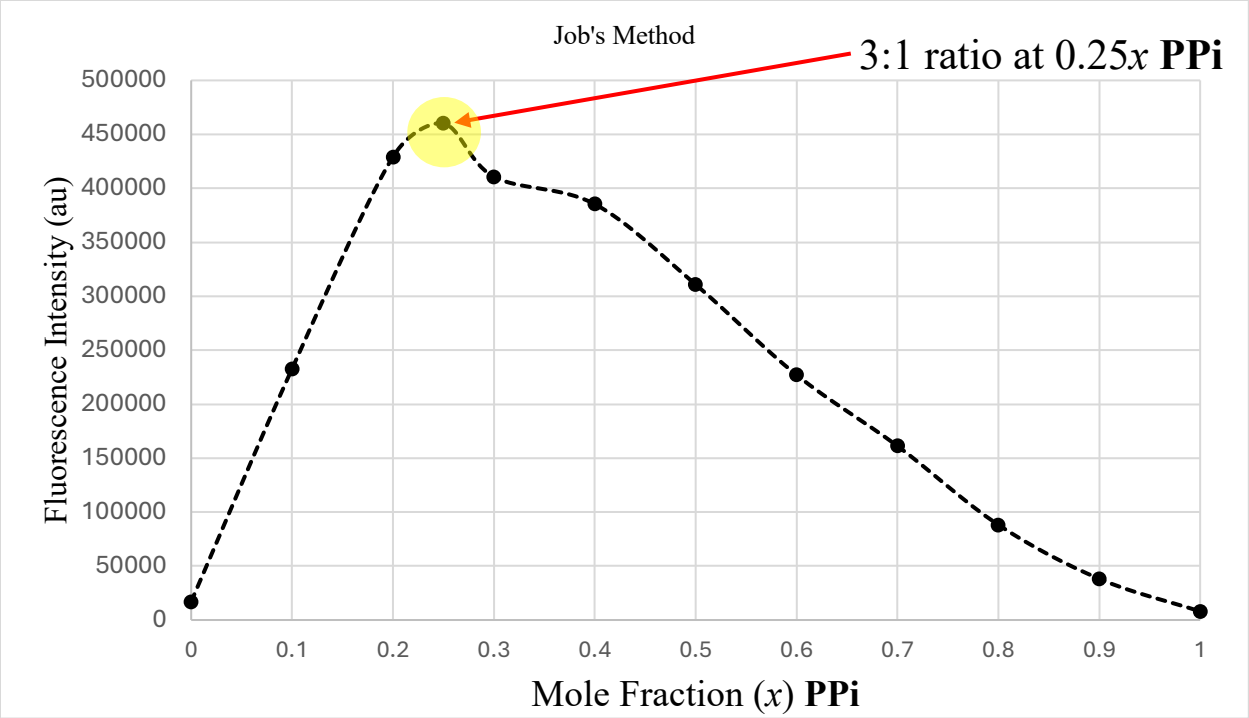

Graph 14.b. A Job Plot analysis for PPi binding to **$ZnCl_2L_4$** (100uM) [excitation 400nm and emissions 520nm] at a 1:3 ratio in HEPES buffer (pH 7.4)

Molar Fraction of PPi	**$ZnCl_2L_1$** (Intensity value /STD Quinine**)**	STD **$ZnCl_2L_1$** (STD **$ZnCl_2L_1$** /STD Quinine**)**	**$ZnCl_2L_2$** (Intensity value /STD Quinine**)**	STD **$ZnCl_2L_2$** (STD **$ZnCl_2L_2$** /STD Quinine**)**	**$ZnCl_2L_4$** (Intensity value /STD Quinine**)**	STD **$ZnCl_2L_4$** (STD **$ZnCl_2L_4$** /STD Quinine**)**
0	0.001213957	0.007852097	0.003463918	0.165369071	0.00012447	0.002177939
0.1	0.001213957	0.007852097	0.003463918	0.165369071	0.00012447	0.002177939
0.2	0.001213957	0.007852097	0.003463918	0.165369071	0.00012447	0.002177939
0.25	0.001213957	0.007852097	0.003463918	0.165369071	0.00012447	0.002177939
0.3	0.001213957	0.007852097	0.003463918	0.165369071	0.00012447	0.002177939
0.4	0.001213957	0.007852097	0.003463918	0.165369071	0.00012447	0.002177939
0.5	0.001213957	0.007852097	0.003463918	0.165369071	0.00012447	0.002177939
0.6	0.001213957	0.007852097	0.003463918	0.165369071	0.00012447	0.002177939
0.7	0.001213957	0.007852097	0.003463918	0.165369071	0.00012447	0.002177939
0.8	0.001213957	0.007852097	0.003463918	0.165369071	0.00012447	0.002177939
0.9	0.001213957	0.007852097	0.003463918	0.165369071	0.00012447	0.002177939
1	0.001213957	0.007852097	0.003463918	0.165369071	0.00012447	0.002177939

Table 2. Job's method data points for **Graph 1.**

Job's Method STD **$ZnCl_2L_1$**	1091441.482
Job's Method STD **$ZnCl_2L_2$**	22986300.84
Job's Method STD **$ZnCl_2L_4$**	298377.5874
Job's Method STD OF Quinine for **$ZnCl_2L_1$**	139000000
Job's Method STD OF Quinine for **$ZnCl_2L$**2	139000000
Job's Method STD OF Quinine for **$ZnCl_2L_4$**	137000000

Table 3. Standard Deviations(STD) for all **$ZnCl_2L$** complexes in the Job's method and the quinine (standard curve).

SOP Titration Study:

MATERIALS:

- 100μM solution of **$ZnCl_2L$**
- 100μM solution of **PPi**
- 0.01M HEPES Buffer (pH 7.4)
- 96 black well plate
- Micropipettes (range 30μL-1000μL)

PROCEDURE FOR MAKING THE 0.01M HEPES BUFFER (pH 7.4) SOLUTION

1. Take 2.3865g of HEPES solid and dissolve in a 500mL beaker with 200mL of nanopure H_2O.
2. Adjust the pH from 5.34 to 7.4 by adding 3-5M NaOH.
3. The transfer to a 1000mL volumetric flask and dilute to line with nanopure H_2O

PROCEDURE FOR MAKING THE 100μM **$ZnCl_2L$** SOLUTION

1. You need to make a solution of terpyridine (**L**) at a concentration of 2.5mM a, by dissolving your solid in methanol in a 10mL volumetric flask.
2. You need to make a solution of $ZnCl_2$ at a concentration of 25mM, by dissolving your solid in methanol in a 100mL volumetric flask.
3. Then take 200μL of your $ZnCl_2$ from step 2, mix with 2mL of **L** in step 1, and dilute with 50mL if HEPES buffer (pH 7.4) in a 50mL volumetric flask.
4. The sonicate the solution in step 3 for 5 minutes to ensure solution in thoroughly mixed.

PROCEDURE FOR MAKING THE 100μM **PPi** SOULTION

1. You need to make a solution of PPi at a concentration of 100μM by dissolving the diphosphate salt solid when HEPES buffer (pH 7.4).

Confocal Microscope Bioimaging

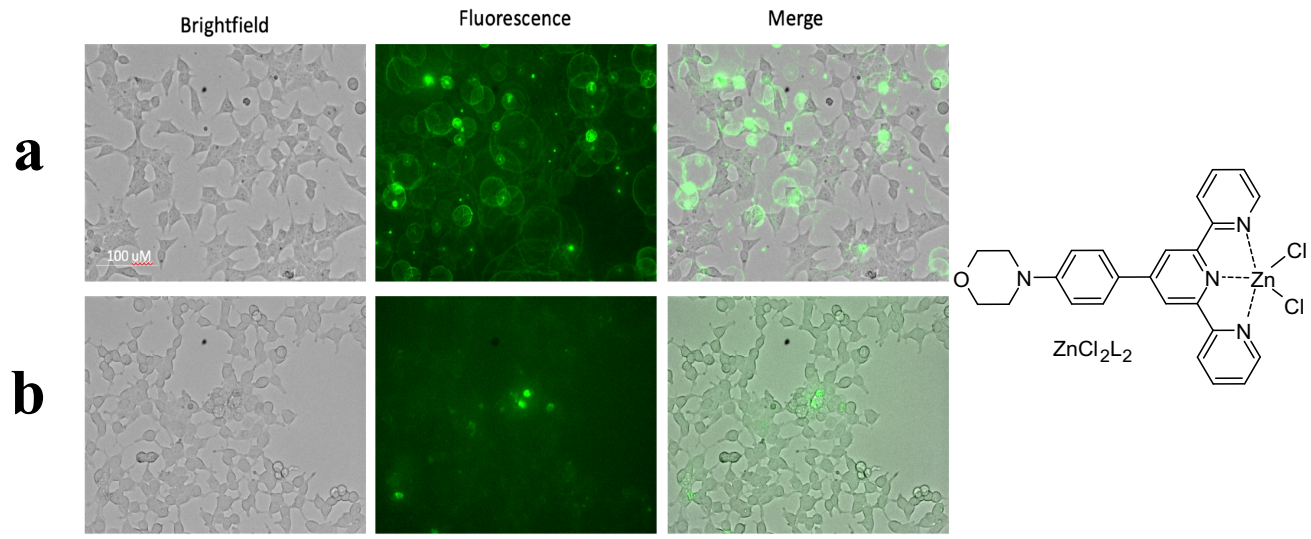

Figure 16. Confocal fluorescence microscope images of 10uM **$ZnCl_2L_2$** incubated in **a)** DMEM for 30mins **b)** HEPES buffer pH 7.4 for 30 mins.

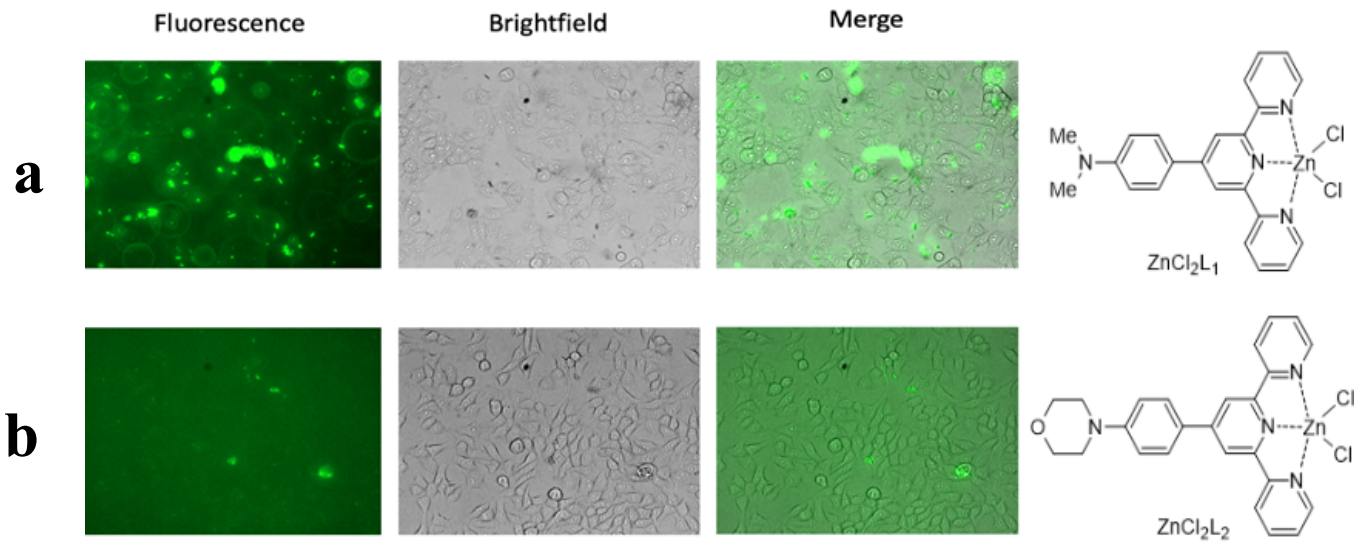

Figure 17. Confocal fluorescence microscope images **a)** 200uM **$ZnCl_2L_1$** **b)** 200uM **$ZnCl_2L_2$** added to HEK293 cells for 30mins in imaging buffer.

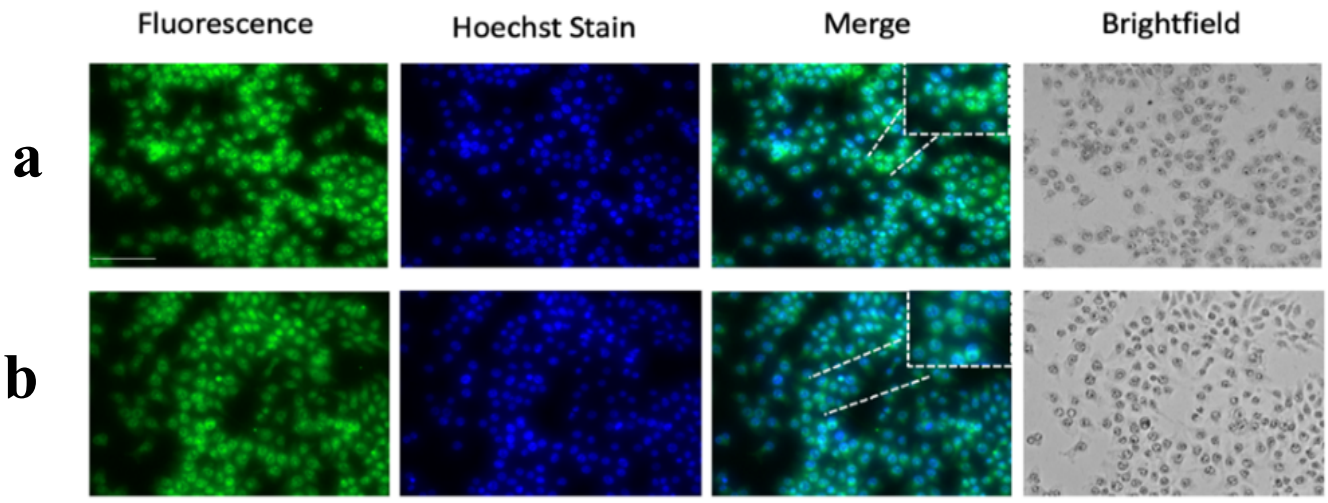

Figure 18. Confocal fluorescence microscope images **a)** 200uM **$ZnCl_2L_1$** 4-(4-dimethylaminophenyl)-2,2':6',2". **b)** 200uM **$ZnCl_2L_{12}$** 4-(4-morpholinephenyl)-2,2':6',2" added to HEK293 cells for 24 hrs. in imaging buffer.

REFERENCES

[1] Lee, D. H., Kim, S. Y., Hong, J.-I., Lee,] D H, Kim, S. Y., & Hong, J.-I. (2004). A Fluorescent Pyrophosphate Sensor with High Selectivity over ATP in Water**. *Angew. Chem. Int. Ed*, *43*, 4777–4780. https://doi.org/10.1002/anie.200453914

[2] J. Am. Chem. Soc. 2014, 136, 5543−5546. Sandip Bhowmik Nanomolar Pyrophosphate Detection in Water and in a Self-Assembled Hydrogel of a Simple Terpyridine-Zn2+ Complex.

[3] Rocco, D., Housecroft, C. E., & Constable, E. C. (2019). Synthesis of terpyridines: Simple reactions—What could possibly go wrong? *Molecules*, *24*(9), 1799.

[4] Bhowmik, S., Ghosh, B. N., Marjomäki, V., & Rissanen, K. (2014). Nanomolar pyrophosphate detection in water and in a self-assembled hydrogel of a simple terpyridine-Zn2+ complex. *Journal of the American Chemical Society*, *136*(15), 5543–5546. https://doi.org/10.1021/JA4128949/SUPPL_FILE/JA4128949_SI_002.CIF

[5] Li, J., Liu, R., Jiang, J., Liang, X., Huang, L., Huang, G., Chen, H., Pan, L., & Ma, Z. (2019). Zinc(II) terpyridine complexes: Substituent effect on photoluminescence, antiproliferative activity, and DNA interaction. *Molecules*, *24*(24). https://doi.org/10.3390/molecules24244519

[6] Latt, SA; Stetten, G (January 1976). "Spectral studies on 33258 Hoechst and related bisbenzimidazole dyes useful for fluorescent detection of deoxyribonucleic acid synthesis". *Journal of Histochemistry and Cytochemistry*. **24** (1): 24–33. doi:10.1177/24.1.943439. PMID 943439

[7] Wongkongkatep, J., Ojida, A., & Hamachi, I. (2017). Fluorescence sensing of inorganic phosphate and pyrophosphate using small molecular sensors and their applications. *Phosphate Labeling and Sensing in Chemical Biology*, 1-33.

[8] Chao, D., & Ni, S. (2016). Nanomolar pyrophosphate detection and nucleus staining in living cells with simple terpyridine-Zn(II) complexes OPEN. *Nature Publishing Group*. https://doi.org/10.1038/srep26477

[9] Driscoll, M. D., Rentergent, J., & Hay, S. (2014). A quantitative fluorescence-based steady-state assay of DNA polymerase. *FEBS Journal*, *281*(8), 2042–2050. https://doi.org/10.1111/febs.12760

10 Wang, S., Chu, W., Wang, Y., Liu, S., Zhang, J., Li, S., Wei, H., Zhou, G., & Qin, X. (2013). Synthesis, characterization and cytotoxicity of Pt(II), Pd(II), Cu(II) and Zn(II) complexes with 4'-substituted terpyridine. *Applied Organometallic Chemistry*, *27*(7), 373–379. https://doi.org/10.1002/aoc.2988

[11] Chu, Q., & Pang, Y. (2006). Terpyridine-substituted, fluorescent polymers and their chelation with zinc ion: The ligand-to-metal ratio and optical properties. *Journal of Polymer Science, Part A: Polymer Chemistry*, *44*(7), 2338–2345. https://doi.org/10.1002/pola.21350

[12] Bencini, A., Bartoli, F., Caltagirone, C., & Lippolis, V. (2014). Zinc(II)-based fluorescent dyes: Luminescence modulation by phosphate anion binding. *Dyes and Pigments*, *110*, 169–192. https://doi.org/10.1016/j.dyepig.2014.04.009

[13] Banjoko, V., Xu, Y., Mintz, E., & Pang, Y. (2009). Synthesis of terpyridine-functionalized poly(phenylenevinylene)s: The role of meta-phenylene linkage on the Cu2+ and Zn2+ chemosensors. *Polymer*, *50*(9), 2001–2009. https://doi.org/10.1016/j.polymer.2009.02.045

[14] Bi, X., & Pang, Y. (2016). Optical Response of Terpyridine Ligands to Zinc Binding: A Close Look at the Substitution Effect by Spectroscopic Studies at Low Temperature. *Journal of Physical Chemistry B*, *120*(13), 3311–3317. https://doi.org/10.1021/acs.jpcb.6b00515

[15] Anbu, S., Kamalraj, S., Jayabaskaran, C., & Mukherjee, P. S. (2013). Naphthalene Carbohydrazone Based Dizinc(II) Chemosensor for a Pyrophosphate Ion and Its DNA Assessment Application in Polymerase Chain Reaction Products. *Inorg. Chem*, *52*, 27. https://doi.org/10.1021/ic4011696

[16] Terenzi, A., Lauria, A., Almerico, A. M., & Barone, G. (n.d.). *ARTICLE TYPE www.rsc.org/xxxxxx | XXXXXXXX Zinc complexes as fluorescent chemosensors for nucleic acids: new perspectives for a "boring" element Received (in XXX, XXX) Xth XXXXXXXXX 200X, Accepted Xth XXXXXXXXX 200X First published on the web Xth XXXXXXXXX 200X*. https://doi.org/10.1039/b00000000x